CGC-IDS

Project CUNIT-2-112Y6580

Qualitative Evaluation of Inclusions In Moderna, AstraZeneca and Pfizer Covid-19 vaccines.

by

UNIT

Submitted 11 Feb 2022

Executive Summary

UNIT was commissioned by EbMCsquared CiC under project UNITC-112980 to investigate the contents of four injection vials (Moderna 01, Moderna 02, AstraZeneca, Pfizer) for any undeclared ingredients that may cause bodily harm.

This report is the submission of initial findings that confirm the presence of graphene compounds in each of the injection vials. Though a quantitative estimate has not be established for the concentration of graphene in the samples, its occurrence is on a high frequency range on an average 2cm transect when counts were conducted on a higher magnification (40x).

TABLE OF CONTENTS

THIS REPORT AND ANY OF ITS ASSOCIATED CONTENTS MARKED BY THE IDENTITY TAG *AUC101* ARE STRICTLY CONFIDENTIAL.

ANY UNAUTHROSISED REPRODUCTION AND OR DISTRIBUTION OF THIS REPORT IS STRICTLY PROHIBITED.

Any reproduction and distribution queries should be directed to

UNIT

At

info@openplatform.uk

DISCLAIMER

This work is an interim report with the presentation of initial laboratory analysis results of Project UNITC-112980.

Further work is ongoing to critically analyse and process these initial results and produce a more in depth analytical and quantitative report.

UNIT takes no responsibility for interpretations drawn by readers of the report.

1. Introduction

The following report is a product of a joint cooperation between EbMCsquared CiC and UNIT in an attempt to identify the undeclared contents of the current vaccines that are being administered to the UK public causing high numbers of adverse reactions and deaths.

1.1. Background

UNIT was commissioned by EbMCsquared under UNITC-112980 to 91 to analyse contents of four vaccine vials and identify if any of the following components were present in these vials – graphene, graphene oxide, parasites, biological filaments.

The four vaccines that form the subject of this first investigation by UNIT belonged to Moderna, Pfizer, and AstraZeneca.

The entire process of collection and delivery is reported in ANNEXE 1A.

1.2. Descriptions of Vials

1.2.1. Moderna 01 Labelling

The manufacturing label had the following information on the vial:

COVID-19 Vaccine Moderna. 020mg/mL Dispersion for injection. COVID-19 mRNA Vaccine (nucleoside modified) Multidose vial doses of .5mL.

Lot-3004737 Exp. 24/01/2022.

The liquid contained in the Moderna bottle was cloudy to naked eye against the sunlight.

1.2.2. Moderna 02 Labelling

The manufacturing label had the following information on the vial:

COVID-19 Vaccine Moderna. 020mg/mL Dispersion for injection. COVID-19 mRNA Vaccine (nucleoside modified) Multidose vial doses of .5mL.

Lot- Lot-3004737 Exp. 24/01/2022.

The bottle weight prior to breaking of the seal was 18.842gm.

The liquid contained in the Moderna bottle was cloudy to naked eye against the sunlight.

1.2.3. AstraZeneca Labelling

The manufacturing label had the following information on the vial:

Covid-19 Vaccine 4 ml, Astrazeneca Injection. Covid-19 Vaccine: (ChAd0x1-S (recombinant)), Intramuscular use. Multidose vial (8x0.5ml doses). 108439/2 Lot-PW40167 Expiry- 01-22. (Figure 2.1)

The bottle weight prior to the breaking of the seal was 12.184g and after the breaking of the seal was 11.803g.

The liquid contained in the AstraZeneca bottle was transparent to naked eye.

1.2.4. Pfizer Labelling

The manufacturing label had the following information on the vial as in figure 1.1:

Figure 1.1. Pfizer vaccine vial

Lot-FC9001 Exp. 09/01/2022.

The liquid contained in the Pfizer bottle was cloudy to naked eye against the sunlight

1.2.5.

1.3. Aims and Objectives of the study

The aim of the study was to identify any solid inclusions in the vials as were undeclared by the manufacturers.

The study was to verify the findings of graphene related compounds such as graphene oxide, graphene hydroxide by Campara (2021) and report any other biological inclusions that may be interpreted as toxic to human body.

1.4. Report Structure and Outline

The vials went through evaluation of contents at four different laboratory sites that are identified in ANNEXE 1B on request and the methodology adopted is presented in Chapter two.

The report presents an in depth analysis of the findings of this project and is divided into five chapters. Chapter one is the introduction, the second chapter is a description and analysis of the methods used for the evaluation. Chapter three presents the results of the analysis, Chapter four is the interpretation, discussions and conclusions of the study. The Bibliography forms the last chapter of the report.

The entire project involved the inputs of experts in individual fields and their names, affiliations and expertise are identified for reference purposes in Annex 2.

2. Methodology

2.1. Vial Descriptions

The secured vials were made of glass and the vaccines contained within the vials were in a liquid form. The different parts of the vial are shown in figure 2.1. Each of these vials were stored at 4°C in the sample storage rooms until the evaluation of their contents took place. Each of the four vials undertook the same process for evaluation.

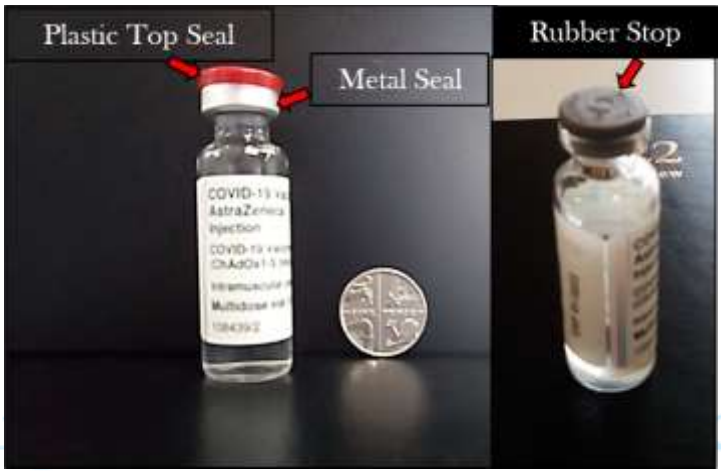

Figure 2-1 Different parts of the sealing process of the vial. The vial shown here is the AstraZeneca vial. The same three seal components were present for the Moderna and Pfizer vials.

2.2. Process of Sampling and Slide Preparation

Stage 1 - Opening of the vial

Stage 1 involved the opening of the vial while the process was recorded on the camera for posterity. Each of the vials were sealed with a plastic seal on the top (figure 2.1). This seal had to be broken off before one could access the rubber top of the injection vial. The rubber top was held securely in place with a metal ring.

There were two options of accessing the liquids from within the vials. One, was to use an injection syringe and draw out the required amount of liquid. However, knowing that the objective of the study was to identify and report any nano graphene particles within the vials, this method of sample acquisition was not thought to be appropriate. The reasoning being, that during the penetration of the vial, the syringe would carry nanoscopic amounts of rubber seal material, which is a carbon product, each time, it would access the liquid. Therefore, the second option of material access was adopted, which meant, breaking off the metal ring and simply removing the rubber seal on top each time the sample material was required.

Stage 2 – Subsampling for evaluation of experimental steps required

Stage 2 had the simple purpose of the first evaluation of the sample. As there was no prior study available at hand to determine the chemistry and the physical properties of the material at hand, a small subsample was used from the vial to be evaluated under a polarising microscope to identify the gross composition of the material of the vaccine and to have a brief understanding of any inclusions if they were present.

Each of the vaccine's active ingredients seemed to have been preserved in a sucrose-salt rich medium. The optical and physical properties of the preserving medium posed a challenge to the identification of the actual inclusions. In addition to being of nearly the same refractive index as the medium, the micro and nano crystalline nature of the expected inclusions rendered an additional impediment to the task of their isolation.

During, wet microscopic evaluation at the dry laboratories, it was noted from the onset, that the denser material settled at the bottom of the slide and got impregnated and encrusted with the medium solution, while the slide was still in the process of wet examination. Additionally, the deposition of the inclusions occurred at different depths within the medium.

Cummulatively, such characteristics, posed a grave challenge to the central objective of the study, in that, isolation of the objects of interest was deemed impossible. The medium masked all signatures of the inclusions by impregnation and encrustation in a manner that the inclusions were completely camouflaged into the background.

These challenges were attempted to be overridden by vacuum filteration. The first attempt at vacuum filteration failed due to equipment failure. This resulted in the loss of the test material. As, at the time of this experiment, the material at hand was quite limited, any further attempts for both vacuum filteration processes were paused.

(It should be noted, that the ongoing continuation of this project will be using checmical filteration to isolate the inclusions from the onset as the current project has given a clear insight into the chemistry of the product.)

Stage 3- Partitioning of sample for clean slide preparation

This stage included the partitioning of sample into two. The clean portions of the sample were stored in a pyrex glass vial which was cleaned using hydrogen per oxide, hydrochloric baths, then rinsed with distilled water. The vials were then sterilised in the sterilisation chamber prior to the transfer of the sample into them.

0.0125ml of sample was then transferred onto clean slides within fume cupboard and left there to air dry at 20°C under a glass chamber.

The dried slides were mounted using glass coverslips and used for microscopic evaluation. It should be noted that none of the prepared clean slides dried out completely even after a few days.

Stage 3- Optical and Petrological Microscopy

Prepped slides were examined under a reflection and transmission light microscope for organic content and petrological microscope for mineral contents.

Microscopic stage involved preparation of several test slides to identify the typical nature of the content.

On representative slides, counts were done along a specific transect. These were then represented on psimpol to get density options on a typical 0.006ml of sample.

Stage 4 – Raman sampling and preparation

Subsamples from original vials were obtained for Raman spectroscopy. These were transferred onto standard slides using sterilised glass pipettes. The slides were left to dry under glass chambers inside a fan heating oven before being taken for examination to the Raman Laboratories.

2.3. Raman Spectroscopy

As most of the observed inclusions belonged categorically to carbon compounds, Raman Spectroscopy was the chosen method for initial identification of the inclusions. All Raman spectra were recorded in air and at room temperature in back scattering geometry using Renishaw in Via Raman spectrometer. A tunable Ar ion laser was used as an excitation source of 488 nm. The laser beam was tightly focused on the sample surface through a Leica 50x LWD microscope objective with a numerical aperture equal to .5, leading to a laser beam diameter of about 2µm. Spectral resolution was about $2cm^{-1}$.

3.Results

3.1. Description of Inclusions

The analysis of all four vial contents identified objects that are similar. For ease of nomenclature and related descriptions per vaccine, these inclusions are illustrated and defined individually below-

The identified inclusions were-

1. Graphene nano ribbons coated with Polyethylene Glycol
2. Graphene Composite Form 1
3. Graphene Composite Form 2
4. Microcrystalline Calcite with Carbonaceous inclusions
5. Graphene Nano Forms with and without fluorescence
    a. Graphene nano objects
    b. Graphene nano scrolls

3.1.1. Graphene Composites in the form of Nano Ribbons

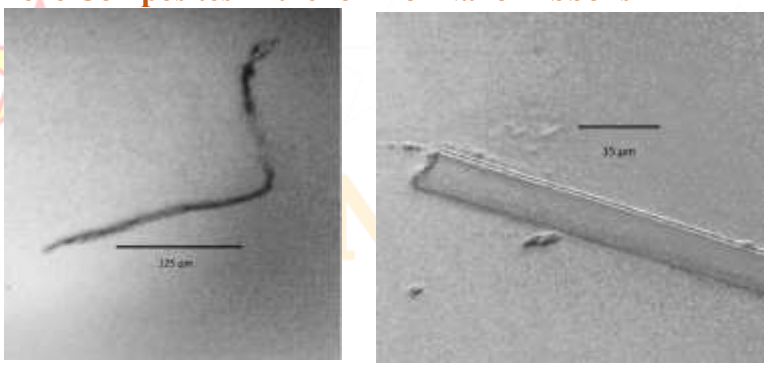

Figure. 3.1. Carbon Composite Ribbon Forms from a sample in Moderna 01. The first picture is of a wet sample and at a low magnification. The second picture is that of the same sample when it is dry and embedded in solution at a high magnification.

This micro inclusion form appears dark grey in wet slides, resembling filamentous ribbons. As the material dries, the form becomes nearly transparent. On high magnifications of 40x, lamellar structures can be identified as sheets. Raman spectrum on these sheets shows a carbon oxygen bond with added polyethylene glycol imprints (figure 3.9). A longer range of the Raman requires to be shot for a better grasp on the distribution of defects and other characteristics of this form.

3.1.2. Graphene Composite form 1

GC1 appears in a translucent folded form of about 10-15microns across. The form is transparent to translucent in transmitted light and shows light structure within it.

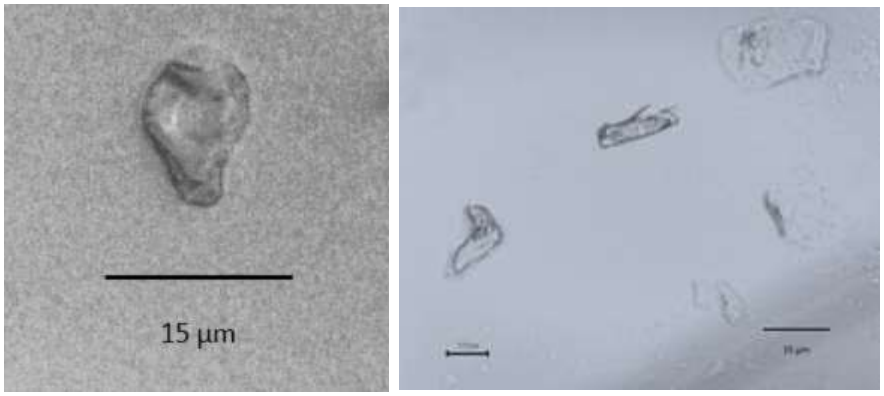

Figure 3.2. An assemblage of different forms with some embedded in the solution appearing translucent and those on the top show a good relief.

GC1 is isotropic under crossed polars. Raman spectroscopic results for this form shows dominant dual peaks of calcite at 1100 cm^{-1} and of some form of iron oxide nearly 500 cm^{-1} . The spectrum beyond 1300 cm^{-1} is quite noisy due to the presence of some fluorescence.

3.1.3. Graphene Composite Form 2

These forms are visibly more intricate and give a rather complex Raman signature. The deciphered components were graphene with iron oxide and calcite. The forms are quite distinct in their lamellar, structure.

The signature for carbon-carbon bond is quite distinct at 1600 cm^{-1} , 1100 cm^{-1} fpeak is picked up for calcite.

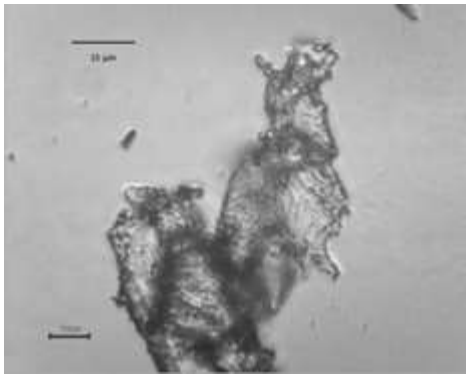

Figure 3.3. Carbon composite Form 2

3.1.4. Calcite

Figure 3.4. Microcrystalline Calcite with graphene inclusions.

Microcrystalline Calcite is another inclusion which is present in the samples. The form can be described as lumpy with inclusions of graphene nano forms. The form gives a very clear Raman signal for Calcite. Calcite is also present in GC1 and GC2 as identified through Raman spectra.

3.1.5. Graphene Nano Forms

Nano forms of graphene were identified in all the samples that were evaluated (figure 3.5). Upon shooting of the Raman when focused on some of these nano objects (in different vaccines), the obtained signals were found to be markedly masked with fluorescence.

Identification of Graphene nano forms was therefore conducted on the basis of microscopic morphological correlation with the forms where, the signal was clear and undebatable (figure 3.24).

Nano forms of Graphene dominated the counts in all the samples. They were found to be present both in roundish shapes and long spiculate shapes. The rounded forms were almost entirely found in association with nano particles.

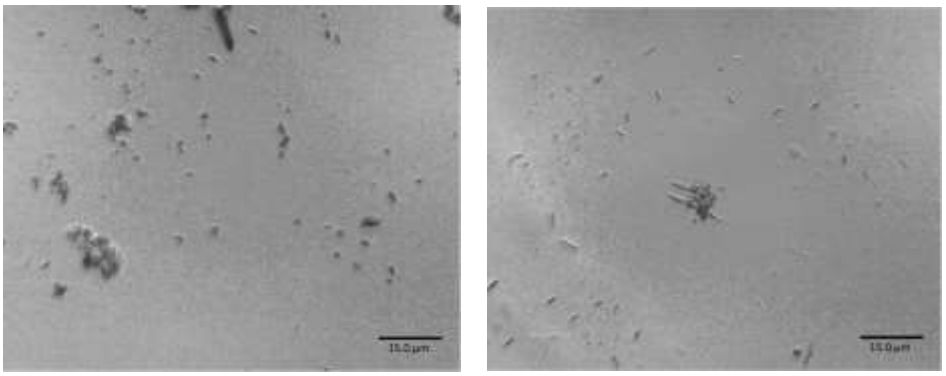

Figure 3.5. (a) Nano forms of Graphene. (b) Nano scrolls.

Quite conspicuously the spiculate forms were noticeably strewn in random orientations at the bottom of all the samples that were examined (figure 3.5).

These nano Graphene spicules were impossible to be evaluated by Raman, as their radius was measurably smaller than the resolution of the laser.

Given, the sheer number of the Graphene scrolls that were noted to be present in the samples, a separate project with the central focus on these scrolls is underway, where, high resolution Raman and invasive FTIR investigations are being undertaken to establish the structures of these scrolls and to get a quantitative estimate of their concentrations.

3.1.6. Crystalised forms of the solution

All the four vaccines are sugar based, and on the edges of the coverslip, as the material dried it crystallised into sugar crystals form in varied shapes. Figure 3.6. shows some varied forms of these crystals under polarised light.

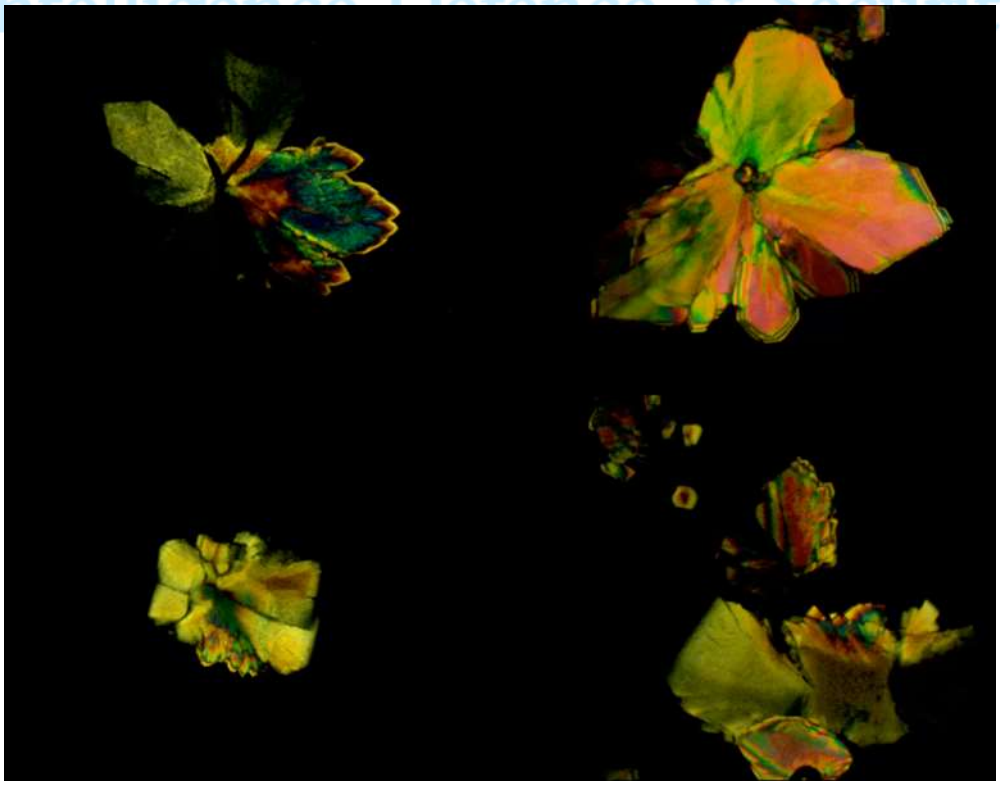

Figure 3.6. Four different forms of sugar base crystals identified in a dried Moderna slide. The crystals display third order interference colours under polarised light with an angular extinction in most cases. The crystals stem from distinctive nucleii.

3.2. Moderna 01

3.2.1. Microscopy

Moderna 01 was the first sample that was evaluated. Under wet microscopy, the sample showed several filamentous forms (figure 3.7). These forms seemed to shed off some of their filaments in form of small flakes (figure 3.7).

As the slide dried, these filamentous forms became incorporated in the solution medium and were optically difficult to distinguish from the background (figure 3.8).

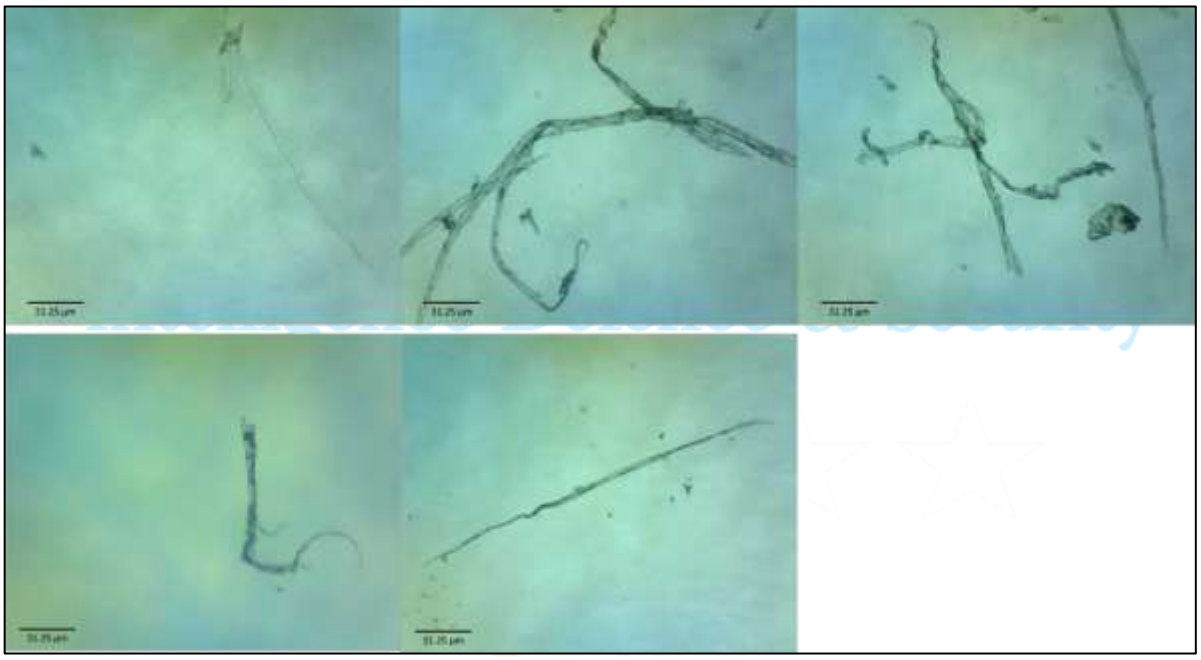

Figure 3.7. Filament forms as observed under wet microscopy.

In the dried state, various forms of particulate inclusions were identified. The settlement of these inclusions took place at multiple levels within the solidified medium. Lighter material came to rest and settle on top and denser material was found at the bottom of the slide.

The crystalised solution seemed to be quite viscous, and it solidified in a thick multi-layered pattern which is quite obvious in form of large sheets with perforations (figure 3.9). On the edges of the slide, the material crystallised into pleochroic crystals stemming from a seed nucleus (figure 3.6). The optical properties of these structures displayed third order interference colours along with the distinct presence of growth nucleus clearly identifying these crystals to be formed of the host solution which includes sucrose.

The ribbon like structures were seen in two states of deposition. One, where partial structure of the inclusion was visible above the solidified medium and part of it was almost transparent and embedded into the medium and the other state was, where the ribbon was incorporated in the medium and was barely distinguishable. The embedded portions seemed to create a quadrilateral geometry with a faint visual signal that seemed like a folded ribbon (figure *3.6*).

Figure 3.8. Ribbon shaped forms half embedded in the medium. Square and quadrilateral crystals in the background.

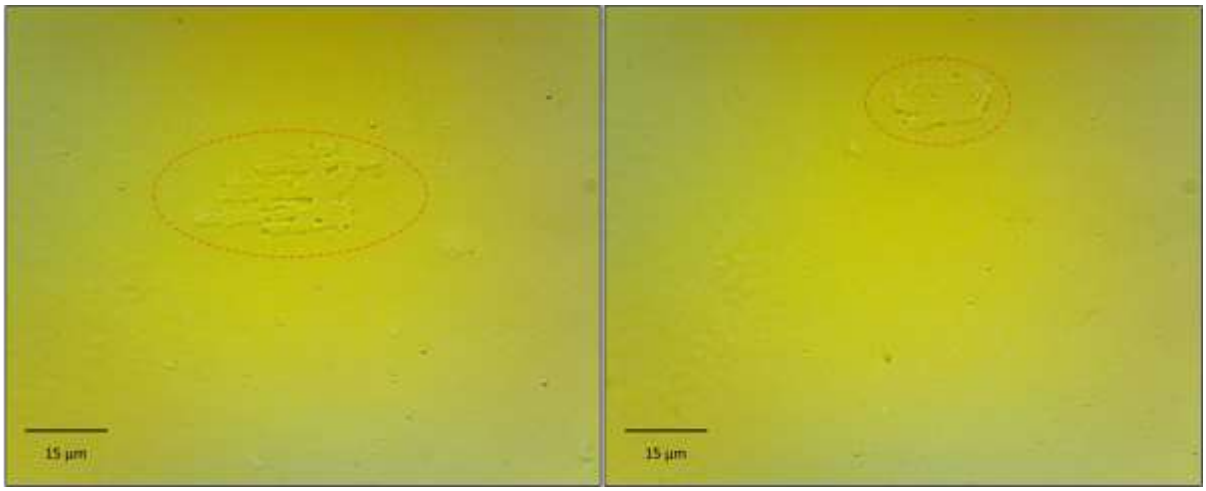

Figure 3.9. Flat, perforated several layered settlements of the medium.

Figure 3.10 exhibits various representative forms that were found in the vaccine. These forms ranged from transparent or translucent sheet like forms, to dark almost opaque amorphous carbon like materials of different sizes (figure 3.10j,k).

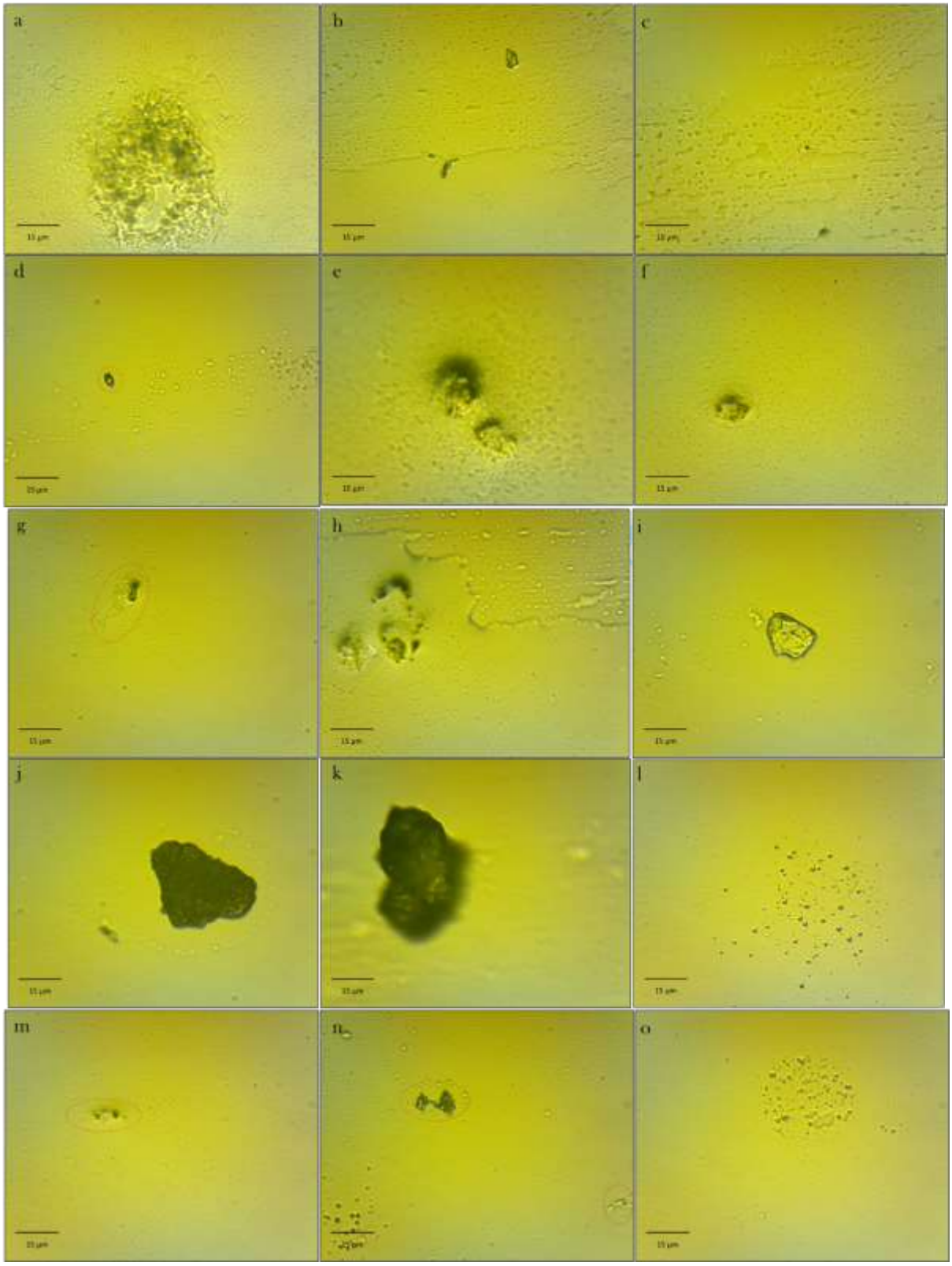

Figure 3.10. Various inclusions found within Moderna 01.

3.2.2. Raman Spectroscopic Investigation

Representative inclusions from Moderna 01 were examined by Raman spectroscopy. The investigation clearly showed that all the inclusions have a strong carbon signal with confirmed graphene compositions of some representative forms.

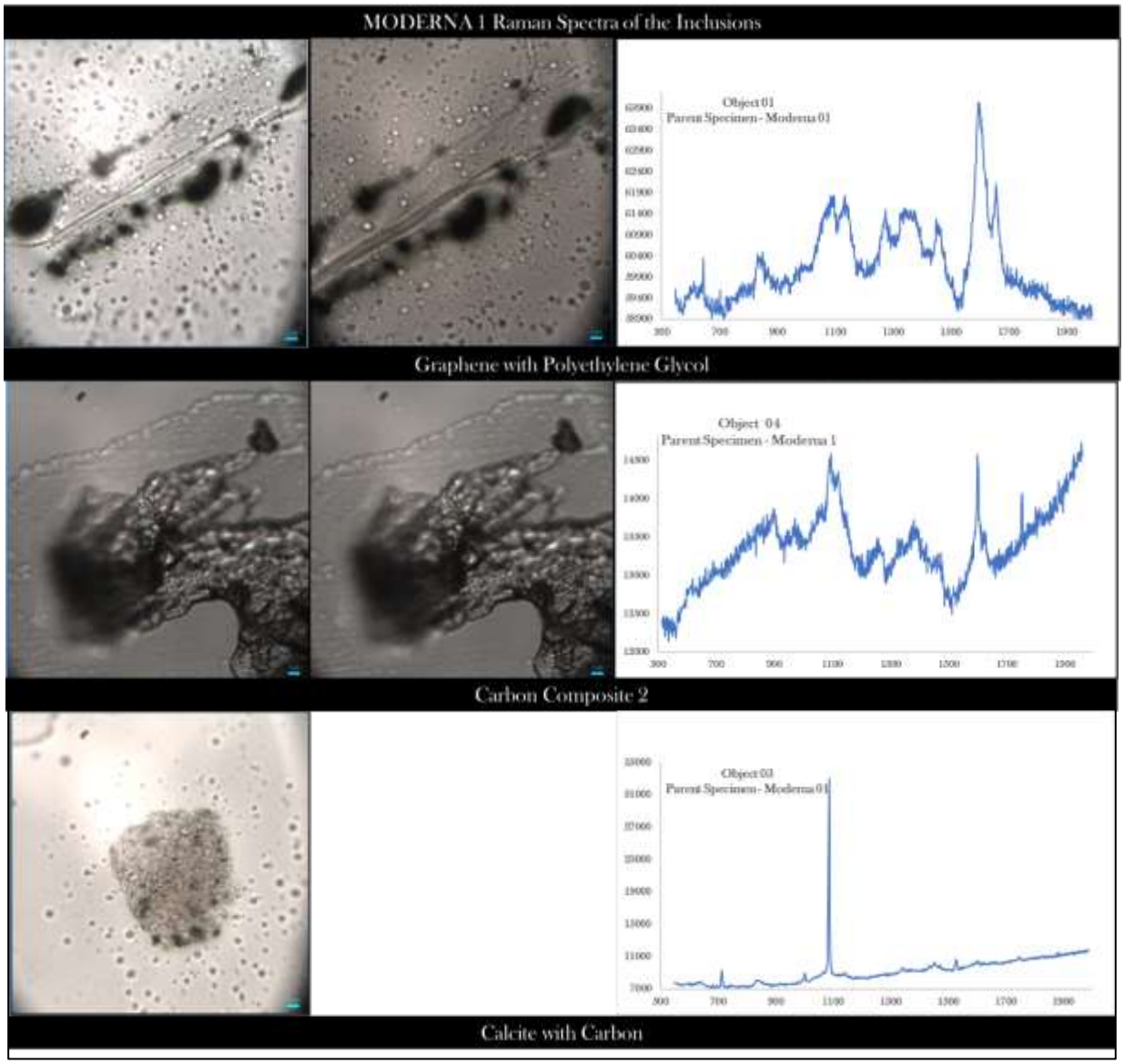

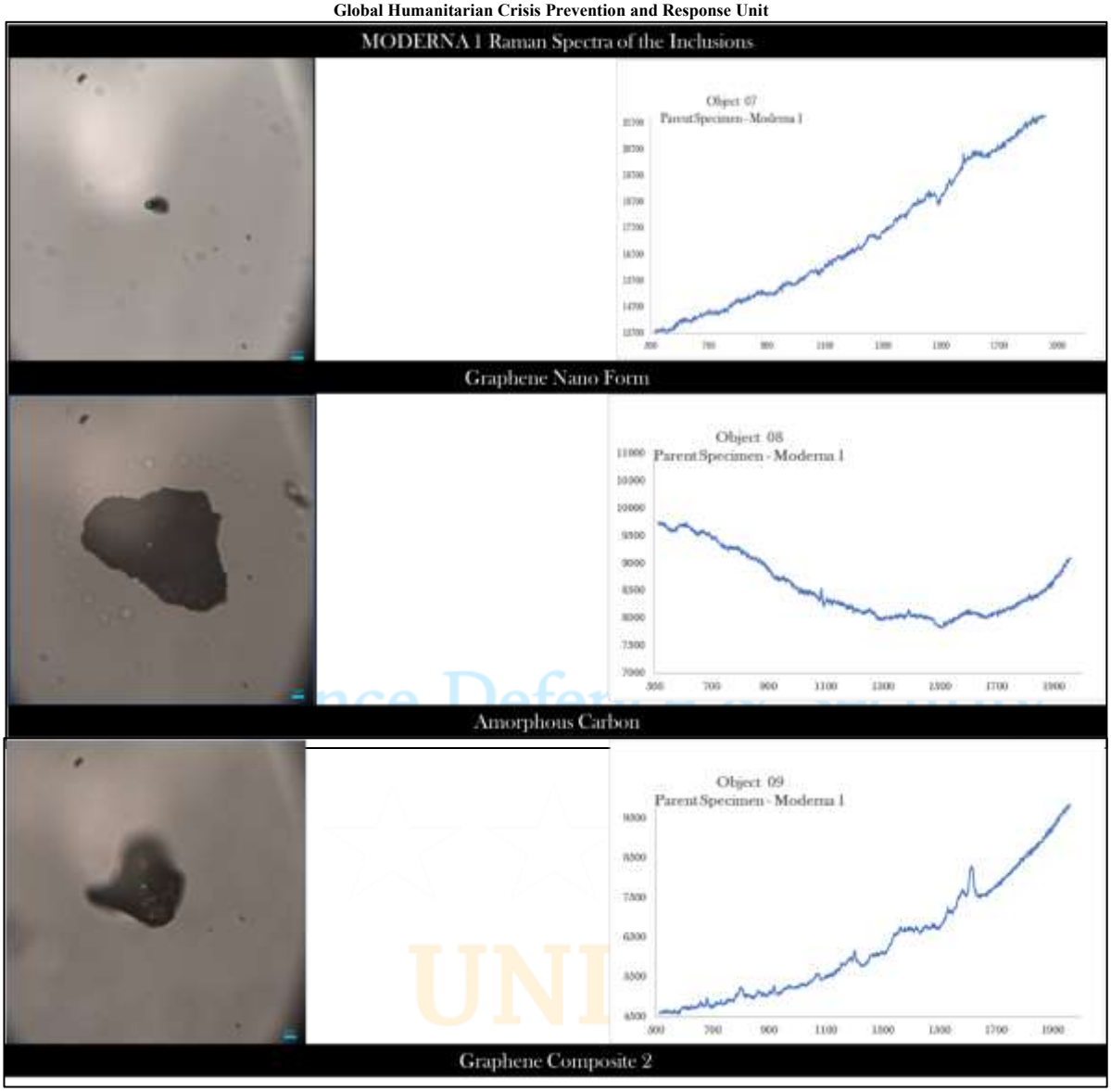

Figure 3.11. Raman spectrum of representative inclusions in Moderna01.

The two clear Raman signals were obtained from two objects. The flat ribbon like inclusions exhibited clear graphene spectra integrated with the spectrum of polyethylene glycol and other minor compounds. The other clear signal was obtained from a calcite microcrystalline form with a distinct strong peak at 1100cm^{-1}.

The carbon composite forms had a highly complicated signal with clear graphene peak at 1600cm^{-1}, but other peaks at 1100 cm^{-1} making the signal quite difficult to separate. Further analysis is currently underway to isolate these signals and identify the other components of this form of carbon. Some nano amorphous carbon forms showed a clear Graphene signal however, these forms also exhibited fluorescence which masked the Graphene peak.

These same forms were identified in other vaccine vials as well allowing for the establishment of their composition consistency across the spectrum of various samples with confidence.

The compositional identities derived of the inclusions through Raman spectroscopy was used to quantify the comparative occurrence of these inclusions along a 2D track. This abundance is presented as counts in the next section.

3.2.3. Counts

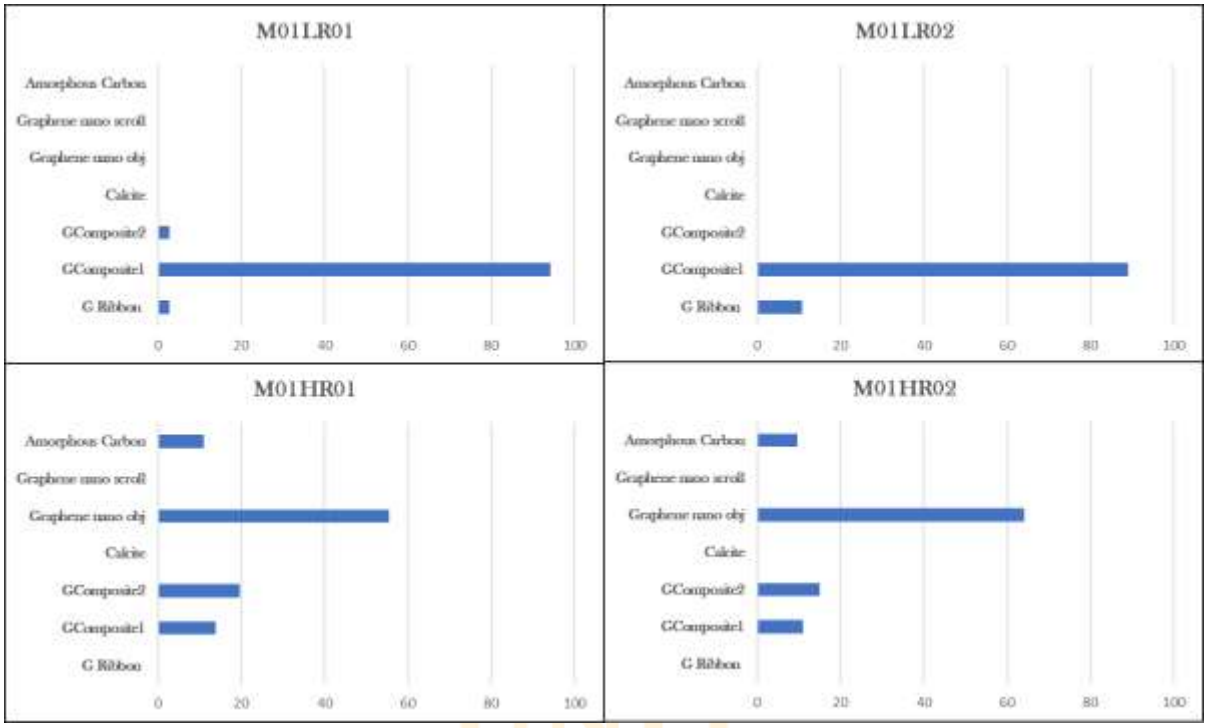

Figure 3.12. Count sheets at low and high resolutions along two tracks each for Moderna 01.

The inclusions were counted along two transects. Each transect was 2cm long. The counts were performed at both: low and high magnifications.

The count distribution is dominated at the low resolution by GComposite 01. At low resolution, GComposite 2 is present in very low quantities, but the abundance reverses at higher magnifications. The counts are overall dominated by Graphene nano objects (figure 3.11).

It should be noted, that Graphene nano scrolls were omitted in the counts. This step was necessary because though, these nano scrolls form a significant percentage of the total counts, a confirmation of their composition could not be attained within the limitations of this project. As mentioned above in Section 3.1.5, thorough investigation of these forms now constitutes the subject of enhanced second investigation project following this report.

3.3. Moderna 02

3.3.1. Microscopy

The sample material from Moderna 2, was translucent on slide with granular particulate material in suspension. On observation of the slide material under wet microscopy, several floating bits of transparent sheet like objects were observed (figure 3.12). Heavier material sank below as traction bedload and salted across the slide while the medium evaporated under the microscopic lamp light.

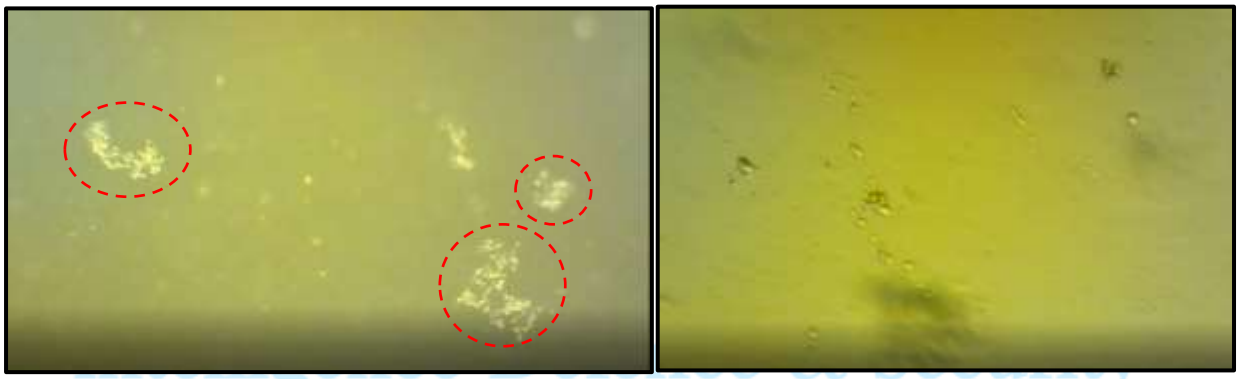

Figure 3.13. Floating sheets of translucent material in a wet sample as observed under an optical microscope. (b) The settled detrital material at the bottom of the slide. The shadows of the lighter floating material can be seen as dark hazy figures.

In regions where the solution column was of a significant thickness, bubbles were observed as flowing with the convection undercurrent towards the edge of the extent of the material. The locus of these particles was clearly striking, even under the lowest magnification.

The graphs obtained by tracking the movement for these particles were typical of self-assemblage systems composed of particles coming together under the influence of various intermolecular forces (figure 3.14).

An interpretation is here drawn in light of the knowledge, that these particles carry the required m-RNA load and under the designated conditions, exhibit the self assemblage characteristics using a combination of non-covalent intermolecular interactions such as electrostatic, hydrophobism, vander Waals and pi effects (figure 3.15).

The self assembly processes seem to be driven by a constantly changing competitive environment which is driven by the kinematic and thermodynamically driven cursours following a typical LaMer model. The seeding of the process seems to be around the nucleic acid form of molecules and Graphene nano objects. According to Kulkarni et al. (2018), the growth of the particle relies on the pH neutralisation and migration of neutral, unbound

ionisable lipid towards the LNP core regardless of the payload (mRNA, minicircular DNA or pDNA).

These particles were observed in ubiquity across the sample preparations and each of these structures began with the formation of a small seed like particle to which the surrounding particles aggregated, based on hydrophobic interactions.

What seems to be obvious through observation is that hydrophobic interactions appear to be the dominant driving force of the LNP growth and electrostatic interactions guide the seed formation and stability of the final assembly.

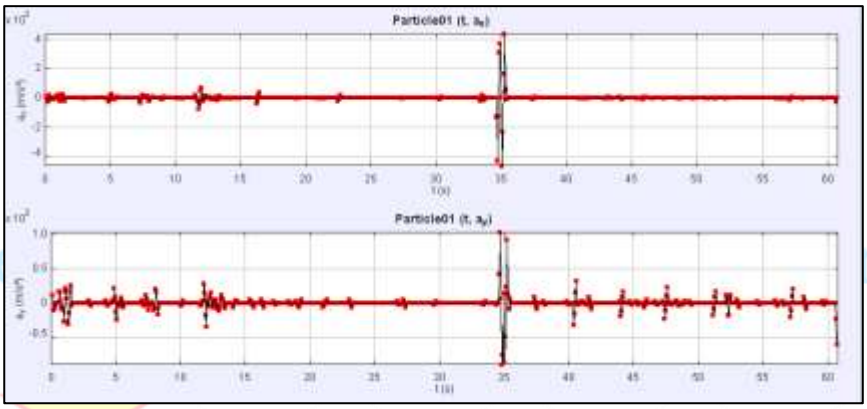

Figure 3.14. Motion graph of a characteristic self-assemblage particle. Accelerations in both X and Y directions show typical staggered forms that typify hydrophobic/philic jumps and movements.

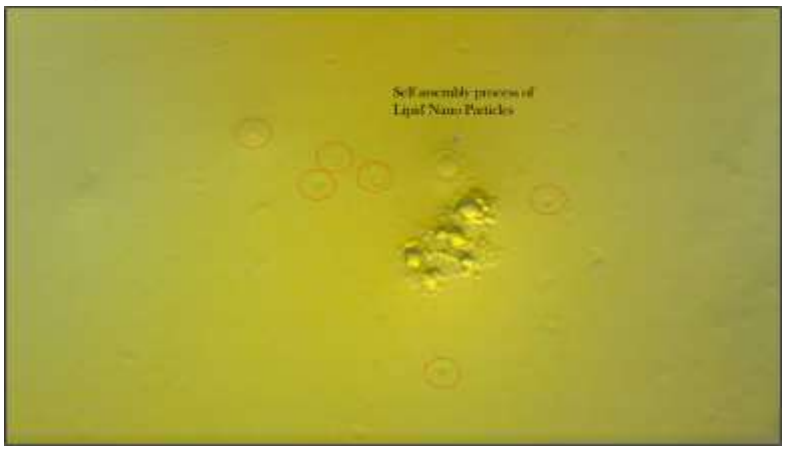

Figure 3.15. Self-Assembled Nano Particles with Payload of mRNA.

On drying of the sample, the solution settled into a thick layer, which retained some form of moisture. The relatively denser material settled to the bottom, while, the lighter material was on the top of the solidified solution with an additional detrital layer in the middle of the medium.

General overview of the dried slide at low resolution exhibited a translucent medium with forms akin to fibres and transparent sheets on the top surface (figure 3.16).

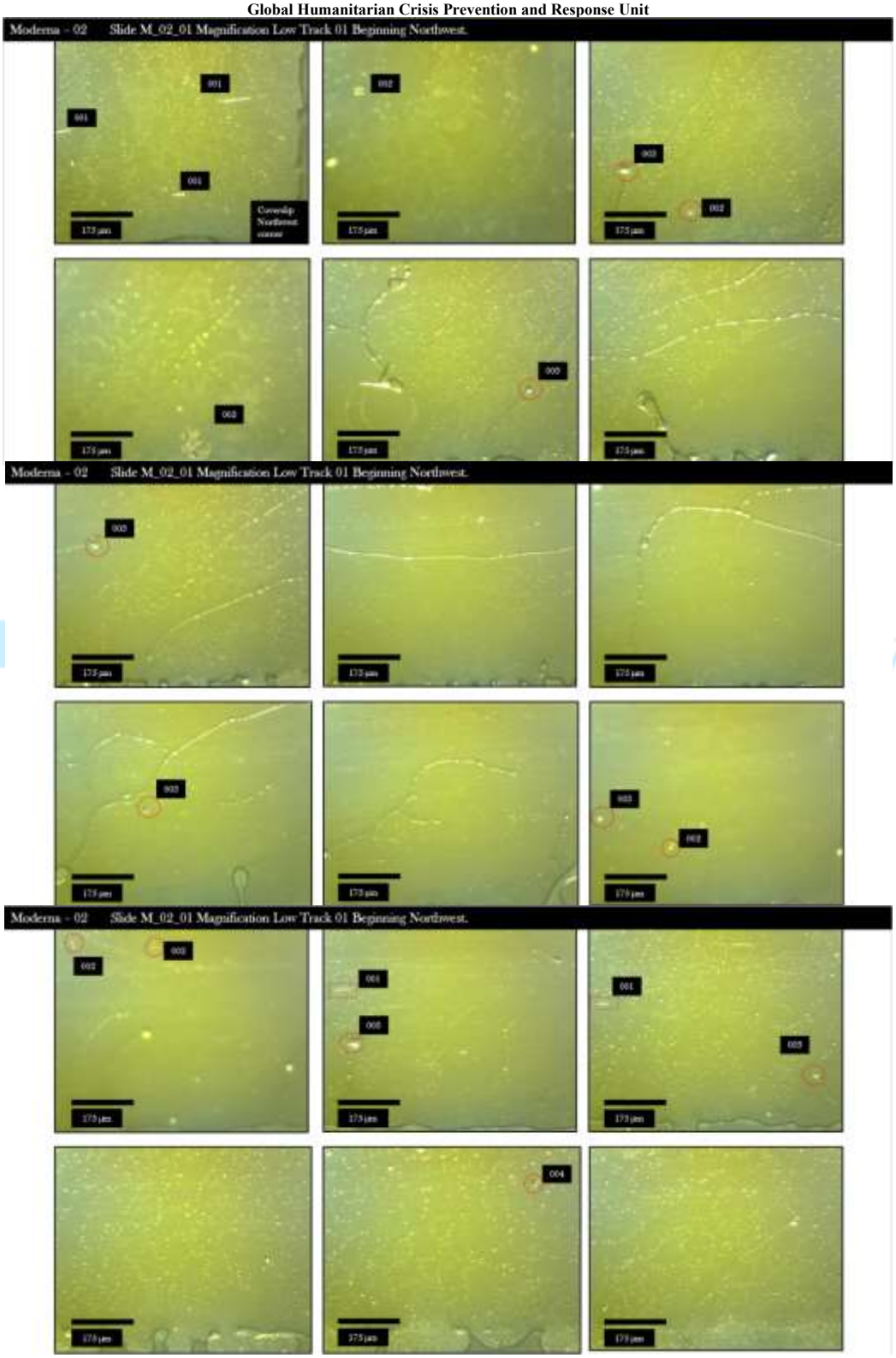

Figure 3.16. Moderna 02 Low Magnification overview of the slide.

On higher magnification, the slide material seemed to abound in carbon-related forms. Figure 3.17 shows different shapes and forms that were noted along various transects across the slide. It is noteworthy, that the noted deposits are on three separate planes, with a significant difference in the depth of focus.

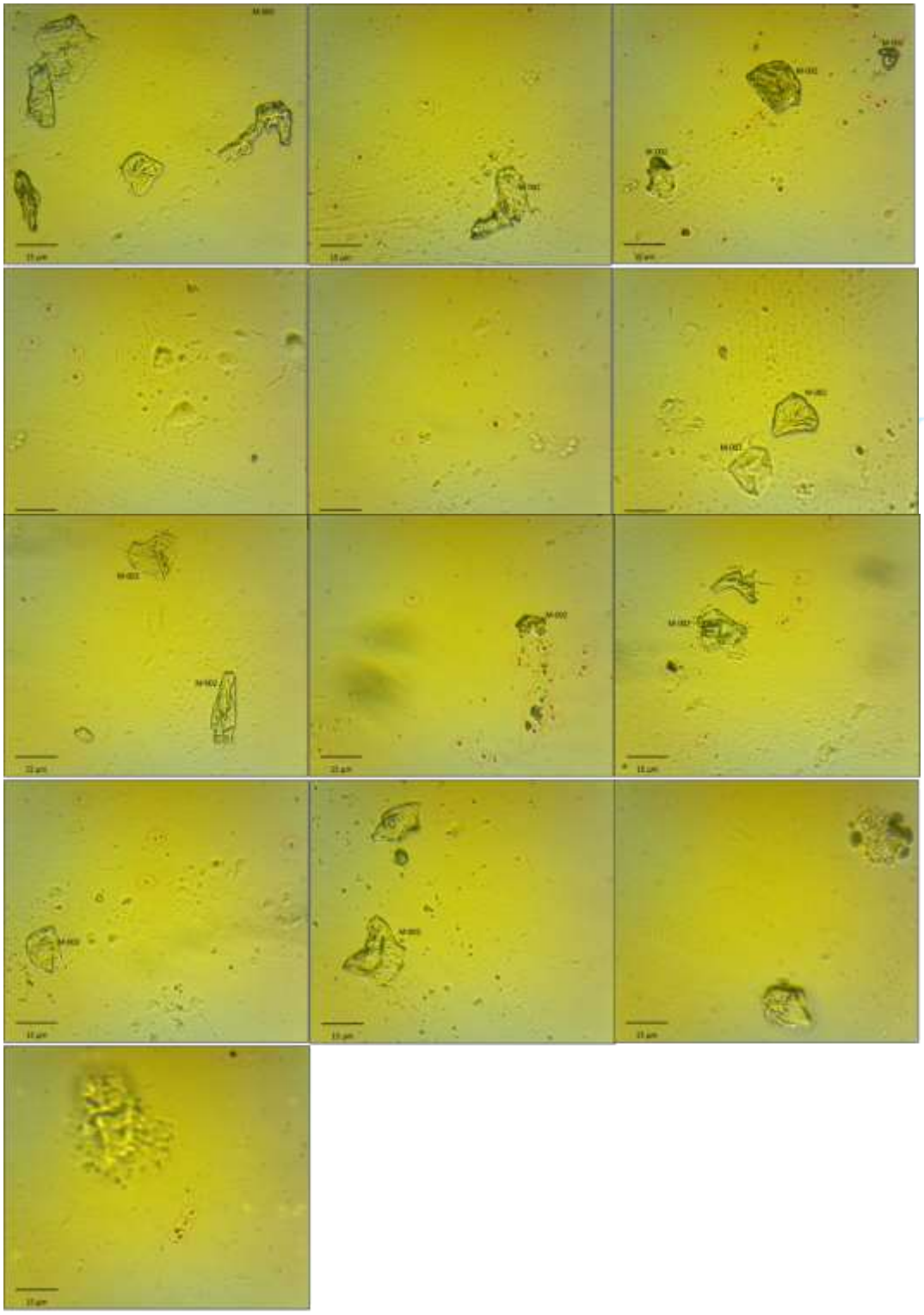

Figure 3.17. Representative inclusions across Moderna 02 at high magnification.

3.3.2. Raman Spectroscopic Investigation

Moderna 2 Raman Spectra of the Inclusions

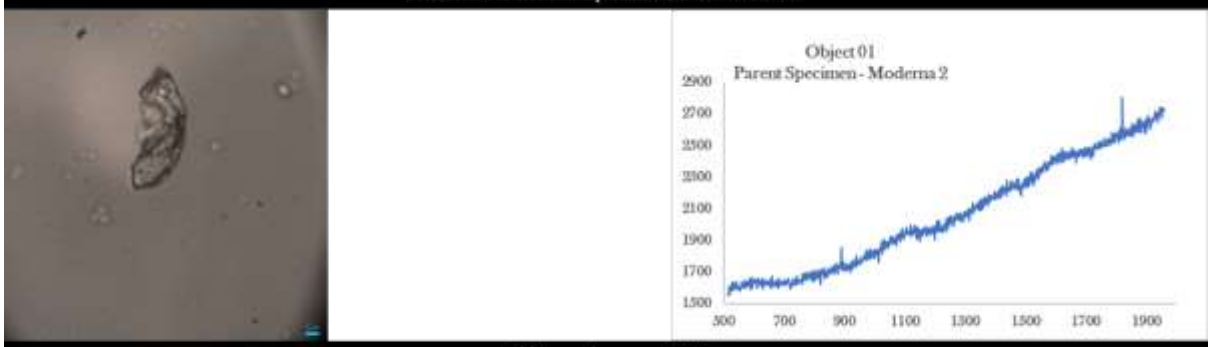

Carbon Composite01

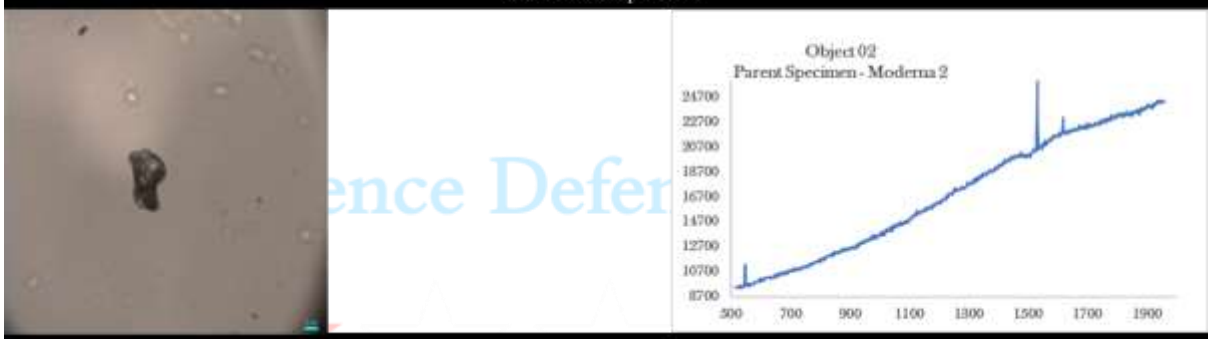

Carbon Composite 02

Moderna 2 Raman Spectra of the Inclusions

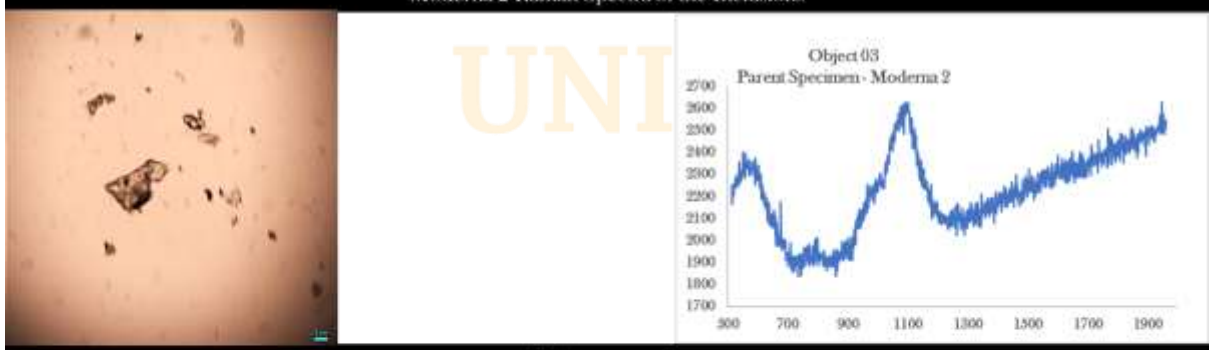

Calcite composite

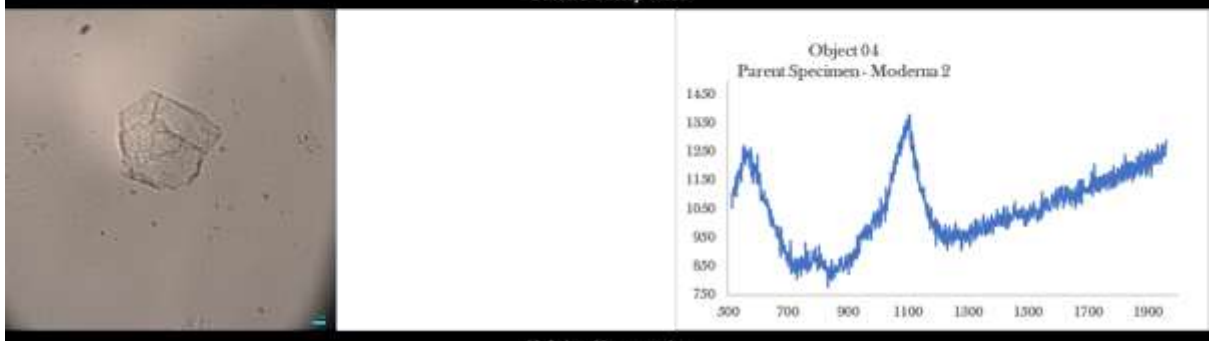

Calcite Composite

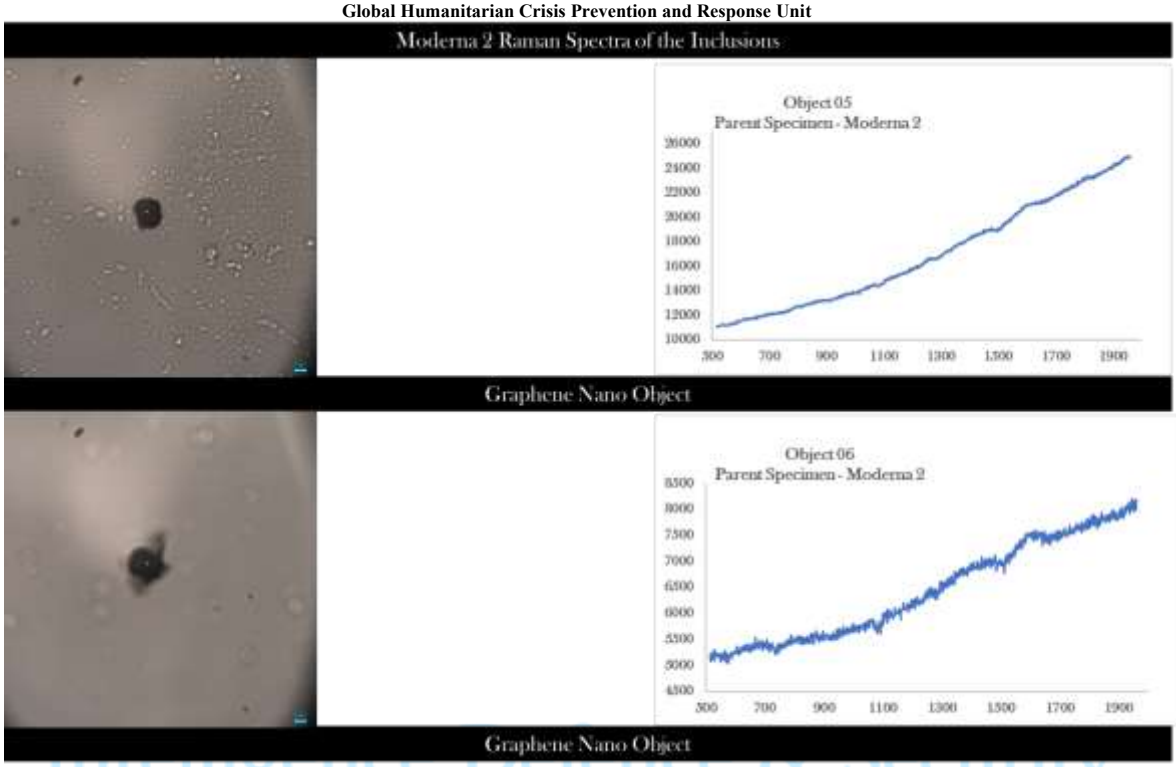

Figure 3.18. Raman spectra of various inclusions in Moderna 02.

Raman spectroscopy was used on the inclusions of Moderna 2 to identify the main representations of the sample (figure 3.18). With the exception of calcite composite samples, the rest showed a highly interfered spectrum. The carbon peaks at around 1600 cm^{-1} and 1350 cm^{-1} were only vaguely discernable in the Graphene nano objects. With the fluorescent background, it was extremely difficult to interpret the spectrum for any other component except carbon.

A reshooting and further processing of the data is highly recommended for these Moderna inclusions to be reasonably identified with some confidence.

In the absence of confident Raman signtures, for analysis of these inclusions, a comparative similarity was used in the presence of the known chemistries of the other inclusions. These chemistries were used to do the counts which are present in figure.

3.2.3. Counts

Counting of inclusions along four tracks of two at low and two at high magnifications showed results similar to Moderna 01 (figure 3.19). Graphene Composite 01 were prominently present

at lower resolution and at higher resolutions, Graphene Nano objects are present in great abundance.

It is clear from the counts, that the nanoscopic structures far exceed the density counts than microscopic structures.

It should be noted, that Graphene nano scrolls were omitted in the counts. This step was necessary because though, these nano scrolls form a significant percentage of the total counts, a confirmation of their composition could not be attained within the limitations of this project. As mentioned above in Section 3.1.5, thorough investigation of these forms now constitutes the subject of enhanced second investigation project following this report.

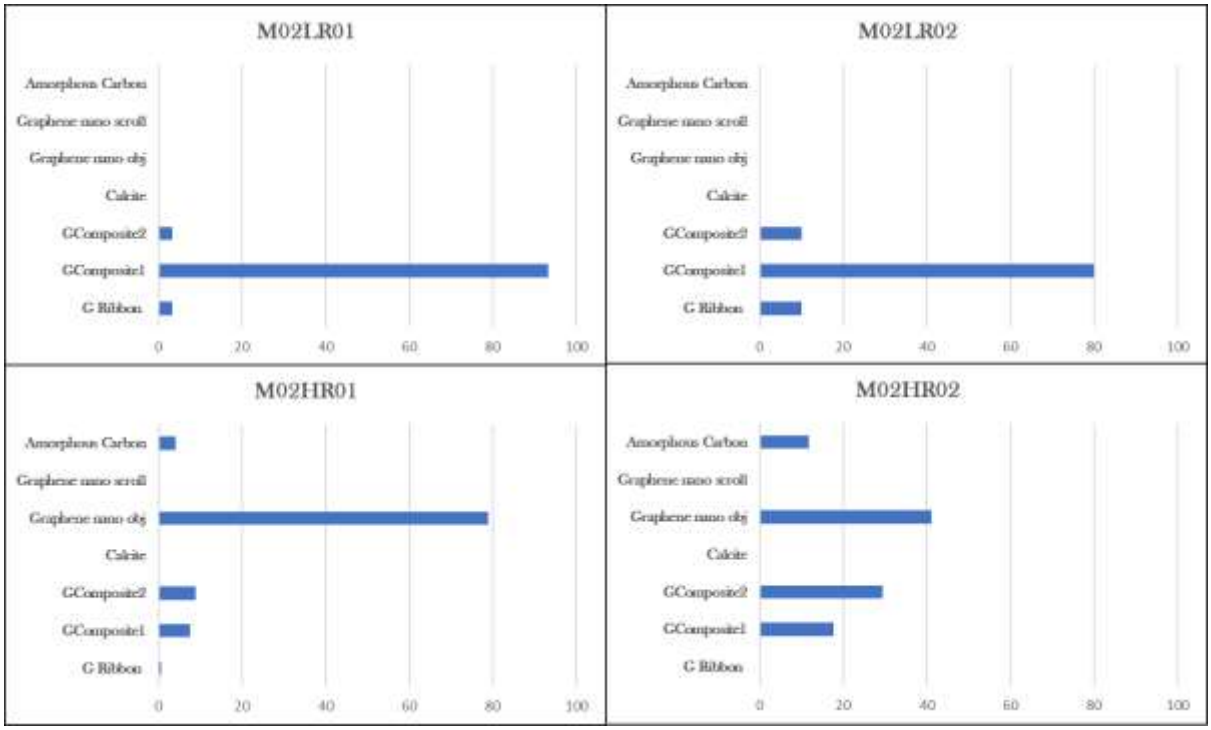

Figure 3.18. Count sheets at low and high resolutions along two tracks each for Moderna 02.

3.4. AstraZeneca

3.4.1. Microscopy

AstraZeneca was the third vaccine that was evaluated for its inclusions. Several fresh runs of the wet samples were seen under the microscope. The AstraZeneca vaccine is almost transparent when seen through the microscope, making the spotting of any inclusions with inherent colours slightly easier.

The wet microscopic observation was that the fresh solution exhibited instantaneous movement of nanoscopic particulate material (figure 3.20) which when observed closely, evolved from being driven by the convection current, to being quite random. As the solution dried up, the particles exhibited traction movement.

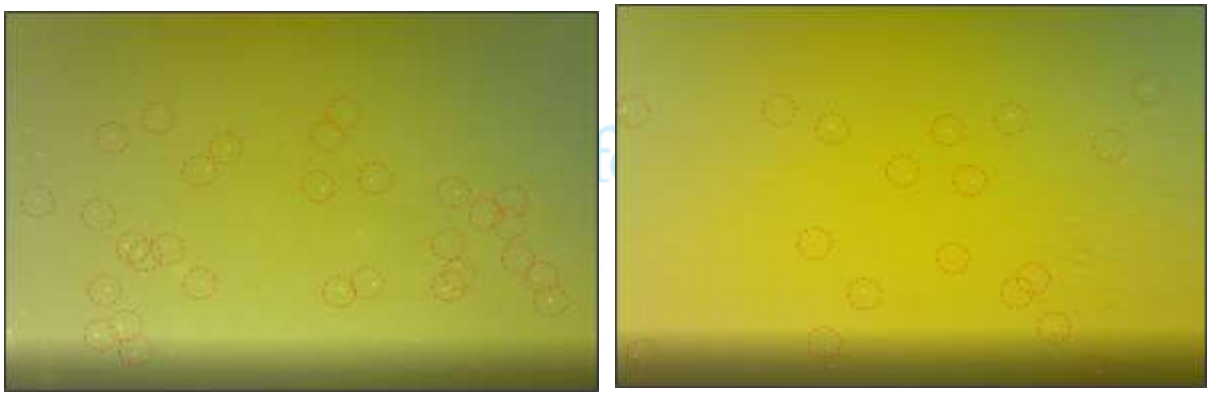

Figure 3.20. Nano Particles in motion when depth of the solution is greater than the height of the particle. The particles coalesce to form bigger particles and the dominating influence on the direction of the movement is through the currents within the solution.

These nanoscopic particles were quite noticeable as white specs in the beginning, as moving in a swarm like motion in the same general direction. With time, these evolved into bigger droplets with more random vectors following the principles of self assembly.

As the solution dried, from the heat of the lamp of the microscope from the top, the sedimentation process began with sheet like forms being deposited on the top of the medium which begins to crystallise early while the liquid below is still able to flow partially. This difference in the crystallisation or solidification pace was clearly discernible from a few slide shots off a video, as are presented in figure 3.21. In the figure, the microscopic form is clearly visible as it is lying on top of the solid film while the nanoparticles are still in motion in the background as can be seen by the shifting position of the shadow. A clear output of this mechanism was that as the medium solidified, it becames more difficult for the nanoparticles to navigate through the viscous material. The core of the nanoparticles was seeded with carbon nanotubes and carbon nano objects: formed of some form of detrital carbon particles. These were dragged along with the eddie currents at the bottom of the medium and as the material

settled, the flute casts were left behind which were identified easily in the dry microscopic sections.

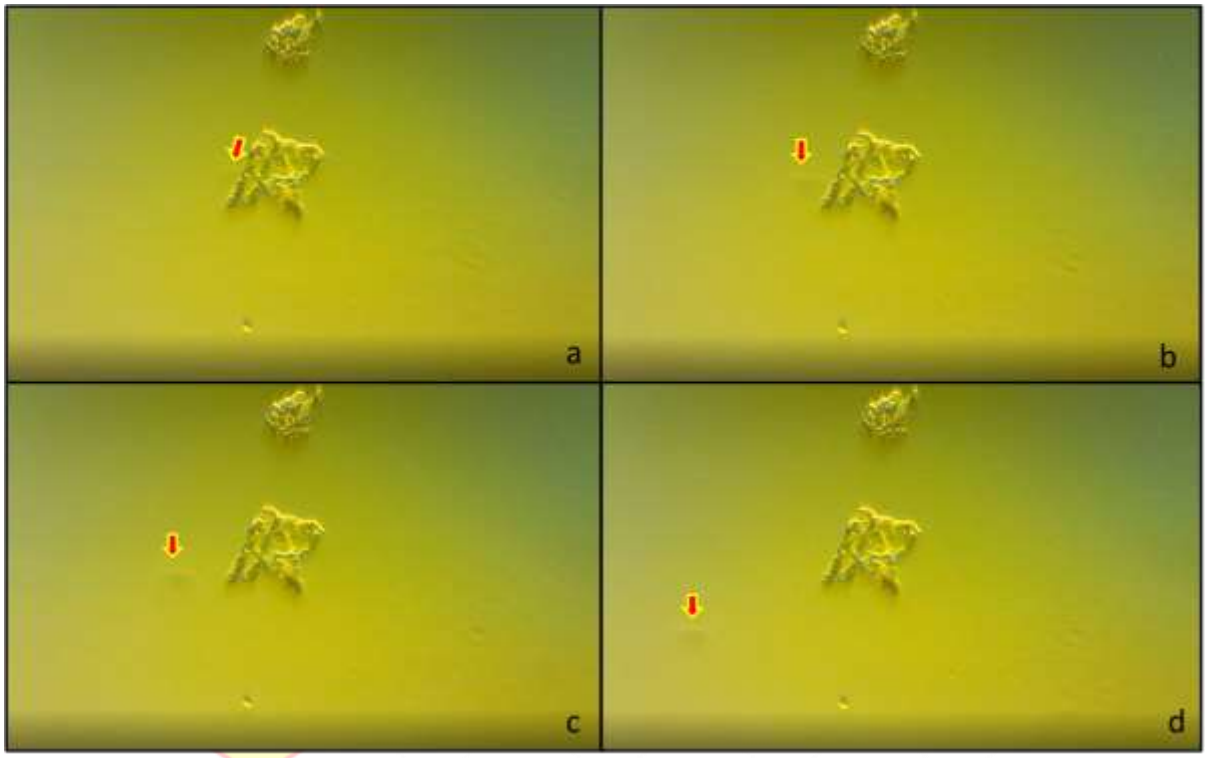

Figure 3.21. Lamellar convection columns with solidified top resulting in deposition of the flaky particle. The arrow points to the position of the nanoparticle in the deeper column of cooler material.

Even, in a wet slide under the microscope, several forms of inclusions were observed. These are described in detail below.

Nano particle movement and self assembly process was noted in AstraZeneca, similar to what was noted in the Moderna vaccines. Here too, the nano particles self assembled through typical signatory movements attributed to the inter-particle forces. While the solution dried up, the heavier carbon material that had sunk to the bottom of the slide was released from the nucleus of the nanoparticles and these now began to exhibit traction movement. Figure 3.22, shows the relative movement vectors of some of these solid materials. When these inclusions settled down, they sank to the lower strata. A later, high resolution examination of the lower strata shows a dump of graphene nano objects (figure 3.23) including graphene nano scrolls (figure 3.24).

Figure 3.22. Distance covered by the object through combined movement vectors

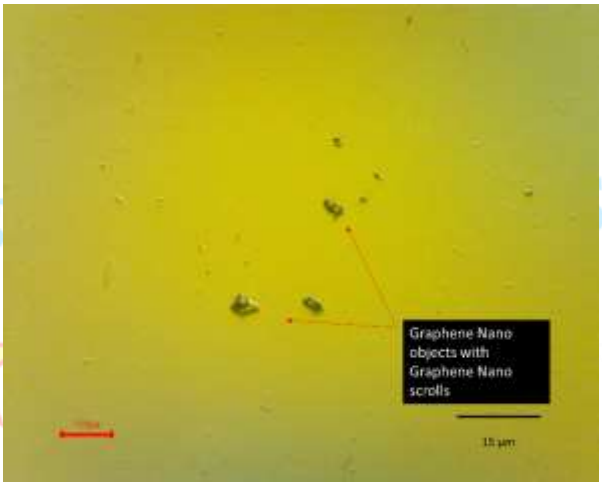

Figure 3.23. Graphene based structures settled down on drying. These structures demonstrated self-movement against the growing viscosity of the drying solution. When the solution dried, they were found to have settled at the bottom of the slide.

Figure 3.24. Graphene scrolls or spicules dumped at the bottom of the slide.

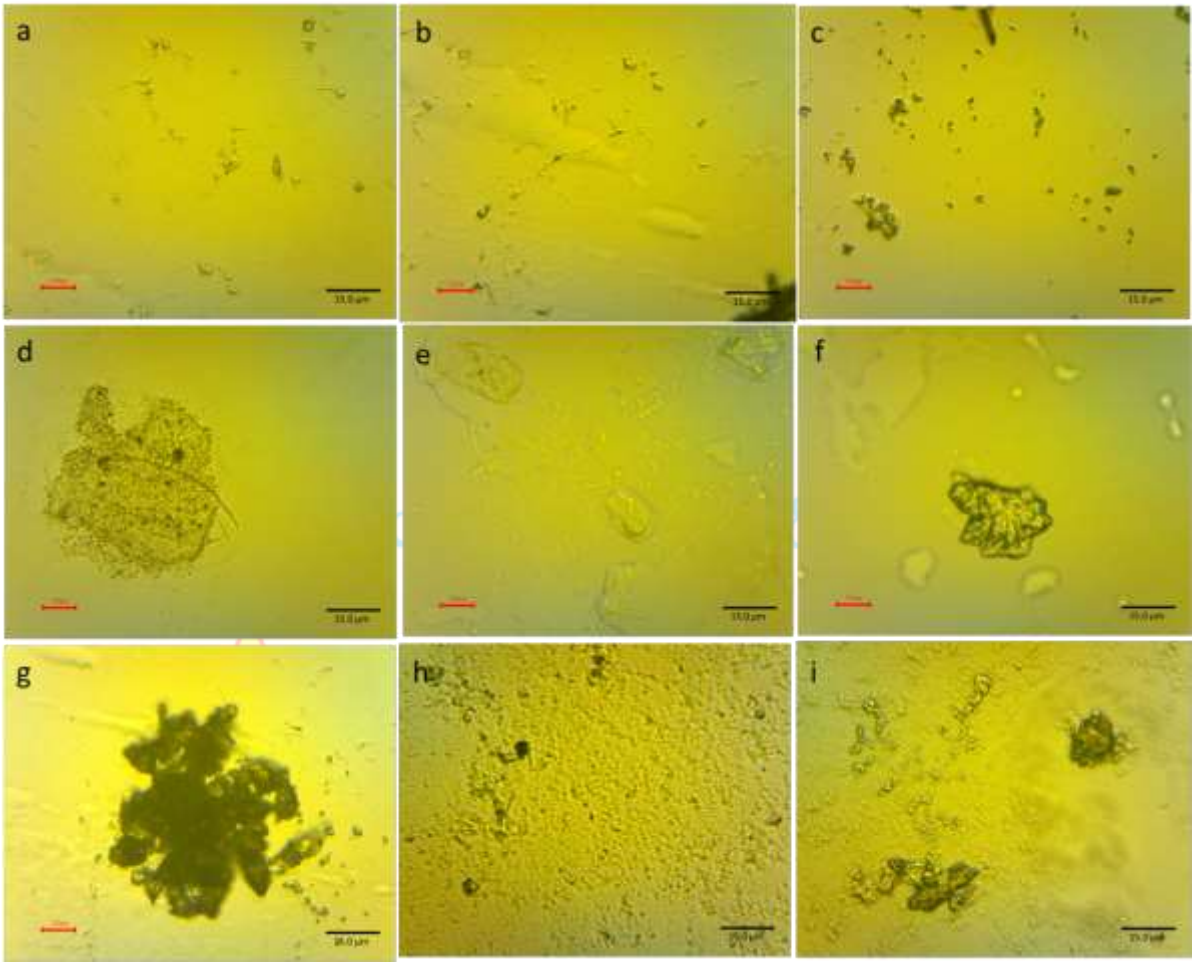

Figure 3.25. Representative inclusions found within AstraZeneca vaccine.

The inclusions identified within AstraZeneca were of the same category as described in section 3.1. These included Graphene composites of two variations, Graphene ribbons impregnated with polyethylene glycol, Graphene Nano Objects including a vast number of nano scrolls and a high count of amorphous carbon. Calcite was also distinctly present in the vaccine in a microcrystalline carbon composite form.

The type inclusions were targeted for Raman identification.

3.4.2. Raman Spectroscopic Investigation

AstraZeneca 1 Raman Spectra of the Inclusions

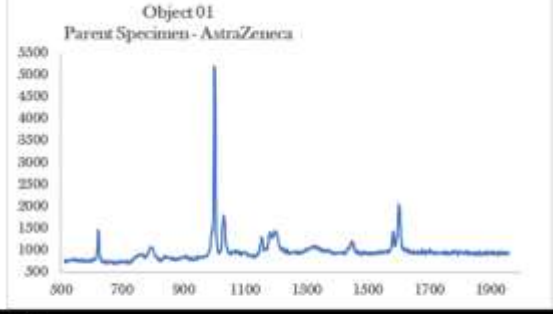

Graphene composite

Carbon Composite

AstraZeneca 1 Raman Spectra of the Inclusions

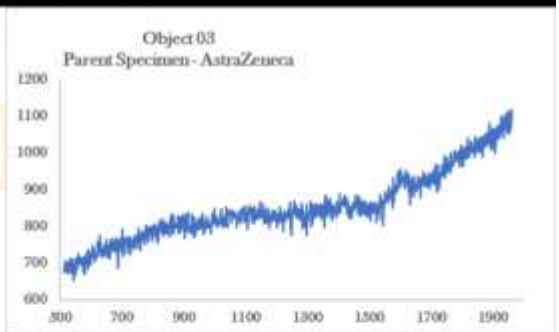

Graphene Composite

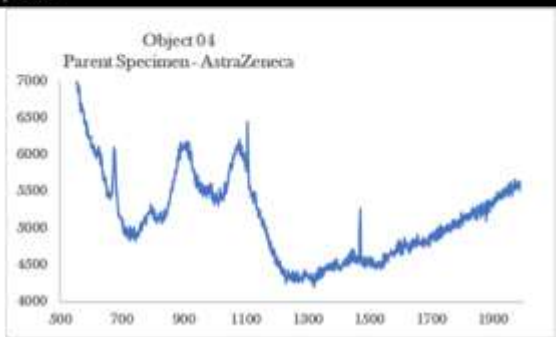

Calcite, Carbon Composite

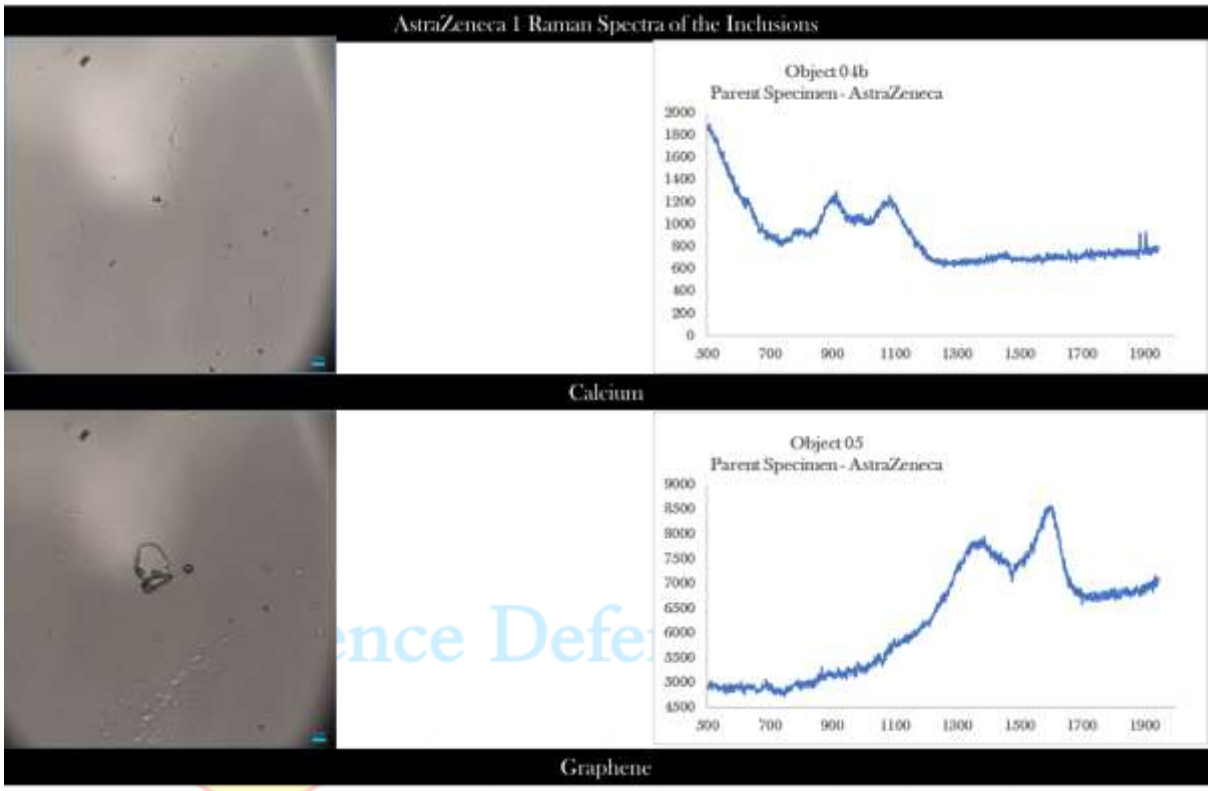

Figure 3.26. Raman spectra of various inclusions in AstraZeneca.

Raman spectroscopy results on inclusions within AstraZeneca yielded direct confirmation of the presence of Graphene in all the identified representative forms.

The carbon composites are of two forms as they are in the Moderna vaccines. These two forms showed distinct graphene signatures through the characteristic Graphene peaks at 1600 cm^{-1} and 1350 cm^{-1}. Besides Graphene, the spectrum is dominated by iron oxide and some other forms of carbon associations.

Further work is ongoing to isolate the signals and help to identify individual compounds. With the exception of one sample of graphene composite, the effect of fluorescence was found to be minimal in AstraZeneca's selected inclusions.

Calcium composites with carbon also showed the same signature as the ones present in the two Moderna vaccines.

The inclusions in the calcite composites contained pristine graphene nano particles. These particles were evaluated to show a clear signal for graphene. Though, the Graphene nano objects were present in clear association with the Graphene nano scrolls, Raman investigations were not carried out on scrolls due to the limitation of the laser size and the microscope's

magnification. In any future work on AstraZeneca, shooting Raman on the scrolls would be one of the main targets in quantifying the concentration of Graphene.

The identification of the inclusions assisted in accurate counting process in the following stage.

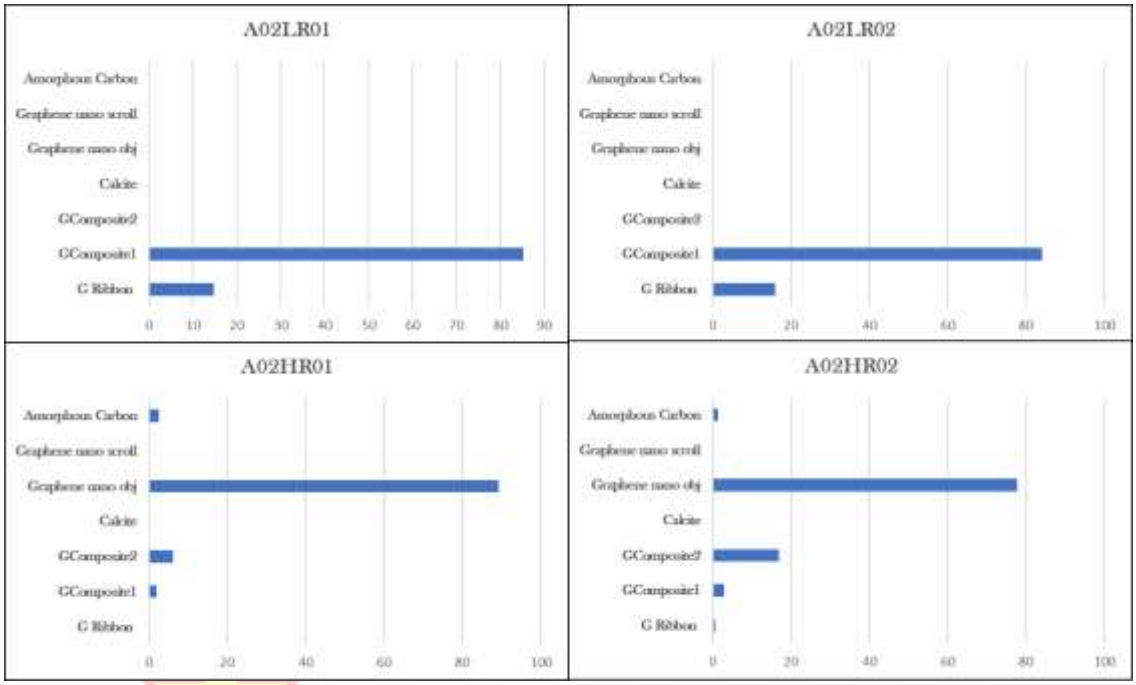

Figure 3.25. Count sheets at low and high resolutions along two tracks each for AstraZeneca.

3.4.3. Counts

AstraZeneca counts do not pick up Graphene composite 2 in the lower magnifications however these are present in significant numbers at higher magnifications. It is clear from the graph that graphene nano objects dominate the count at higher resolutions.

It should be noted, that Graphene nano scrolls were omitted in the counts. This step was necessary because though, these nano scrolls form a significant percentage of the total counts, a confirmation of their composition could not be attained within the limitations of this project. As mentioned above in Section 3.1.5, thorough investigation of these forms now constitutes the subject of enhanced second investigation project following this report.

3.5. Pfizer

3.5.1. Microscopy

Pfizer was the fourth vaccine vial that was evaluated for its inclusions. The vaccine was noted to be of the same offwhite colour as Moderna. 0.006 µL of the sample was transferred on the slide for wet evaluation and an equal amount was left in a slightly inclined pippette to allow for examination in a closed environment in 3dimensions.

The pippete specimen showed some extremely interesting inclusions which were not found when the slide dried. As the material was sucked into the pipette, distinct translucent to transparent sheets were seen floating about (figure 3.28). These were recognized from previous observations in AstraZeneca and Moderna to be the Graphene Composite 1.

Active sedimentation of the denser material on the bottom curve of the cylinder was noted immediately afterwards (figure 3.29).

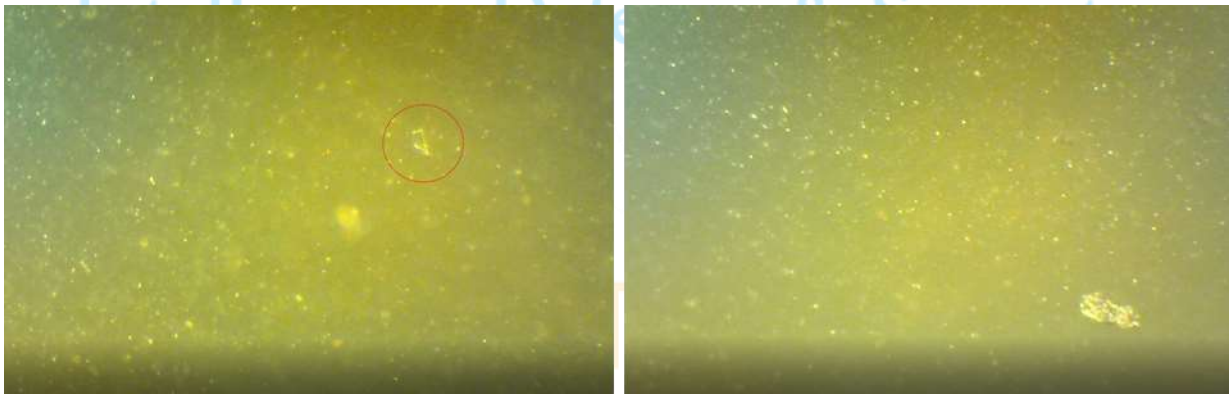

Figure 3.28. Floating lighter material. In the background, the golden sparkly particles are the future self-assembly nano particles that will encapsulate the mRNA.

The two objects of interest that were clearly noted to be floating about but could not be located once the slide had dried, were: (1) an extremely pointy transparent spicule like object (figure 3.30) and the other was a thin translucent perforated sheet (figure 3.31).

Where, both the objects are of interest to this study, the nature of the spicule remains vital for future work to identify.

As the solution was poured onto a slide for observation, the mixture exhibited the same nanoparticulate self assembly mechanism as was observed in both Moderna and AstraZeneca vaccines. As the material dried out, the inclusions settled at various depths depending upon their relative densities.

Figure 3.32 shows an assembly of various forms of inclusion that were identified within Pfizer. These fall in the same category as mentioned in section 3.1.

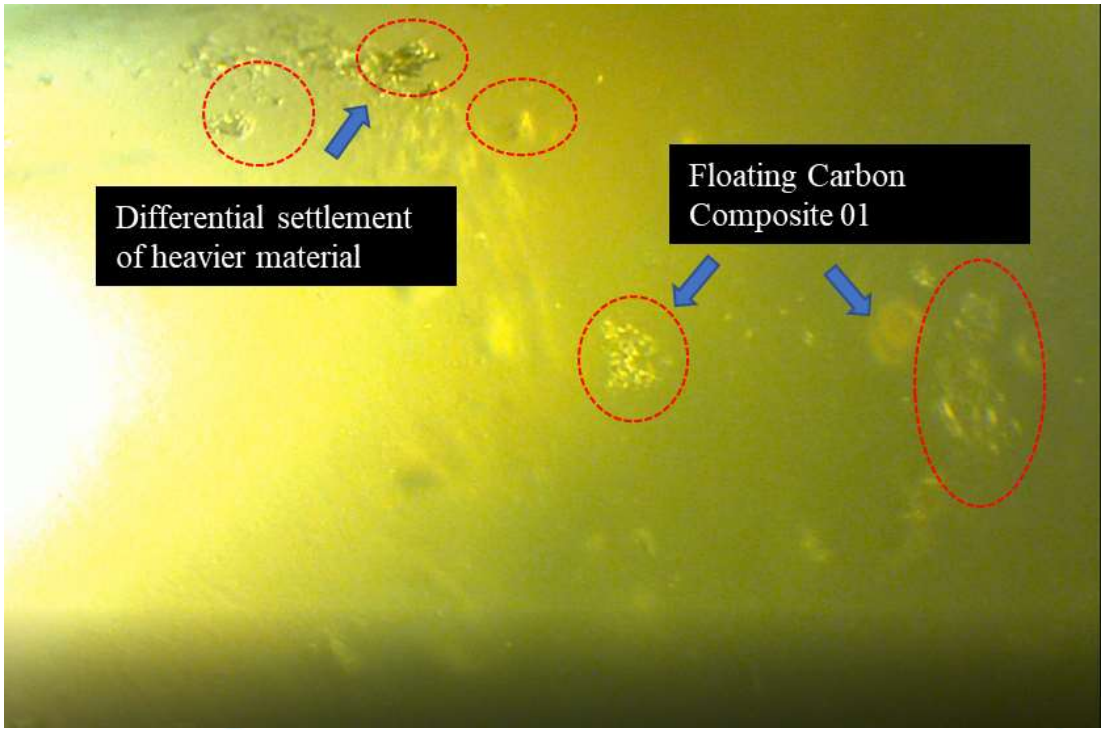

Figure 3.29. Sedimentation of the heavier load on the curved bottom of the pipette and the floating transparent composite 01.

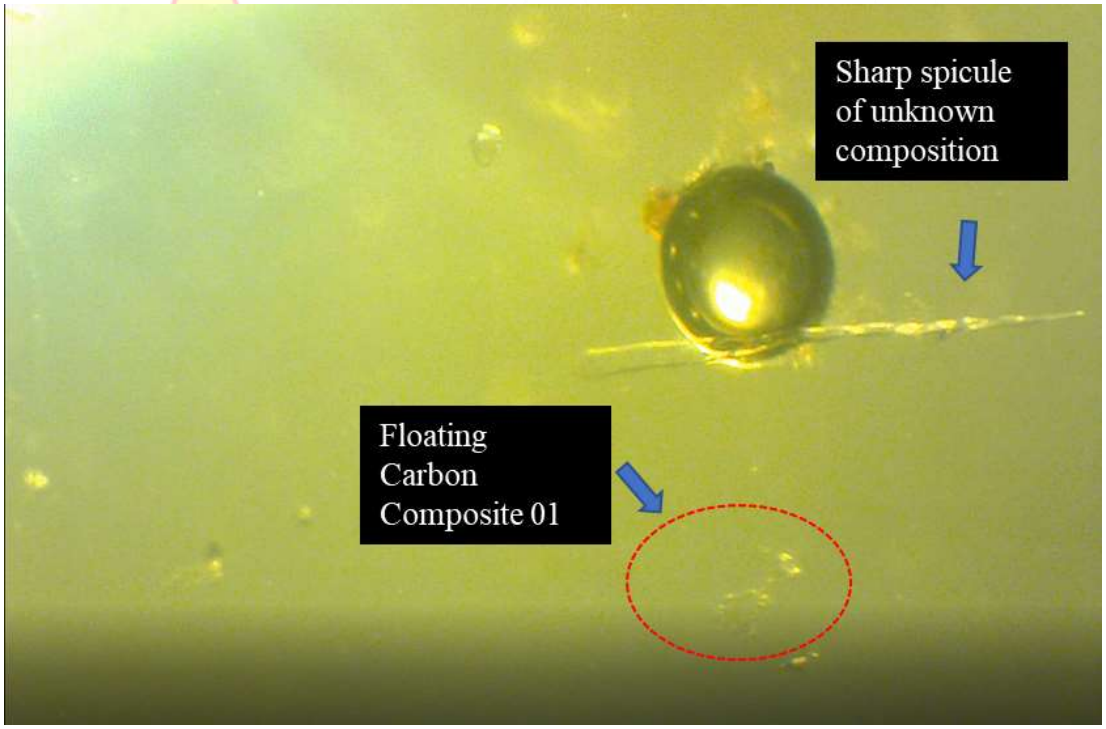

Figure 3.30. Sharp transparent spicule floating in the liquid.

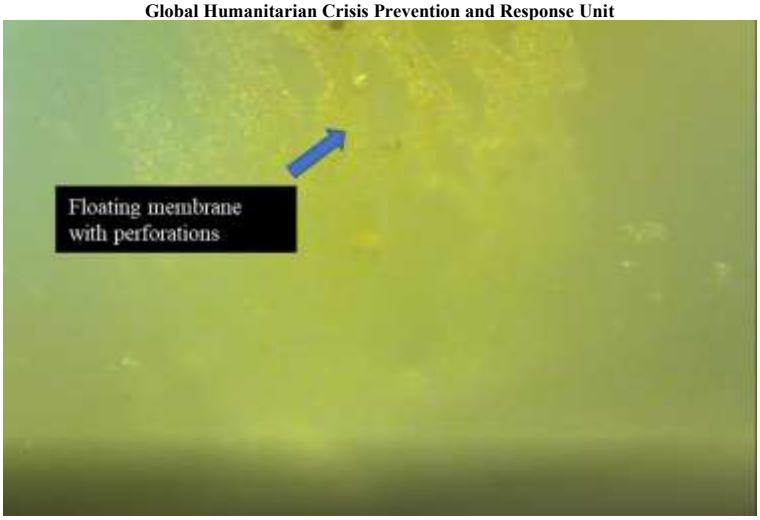

Figure 3.31. Floating perforated membrane.

Ribbon forms of nearly transparent microforms are found in fair number in the slide. These are often half embedded in the solution with one end projecting outside the material.

The carbon composites of both form 1 and 2 also are present in great numbers. Form 1 settles on top of the material while form 2 is found at mid levels of the solidified medium.

Graphene nano forms are present in fair numbers within the slide material along with some scrolls.

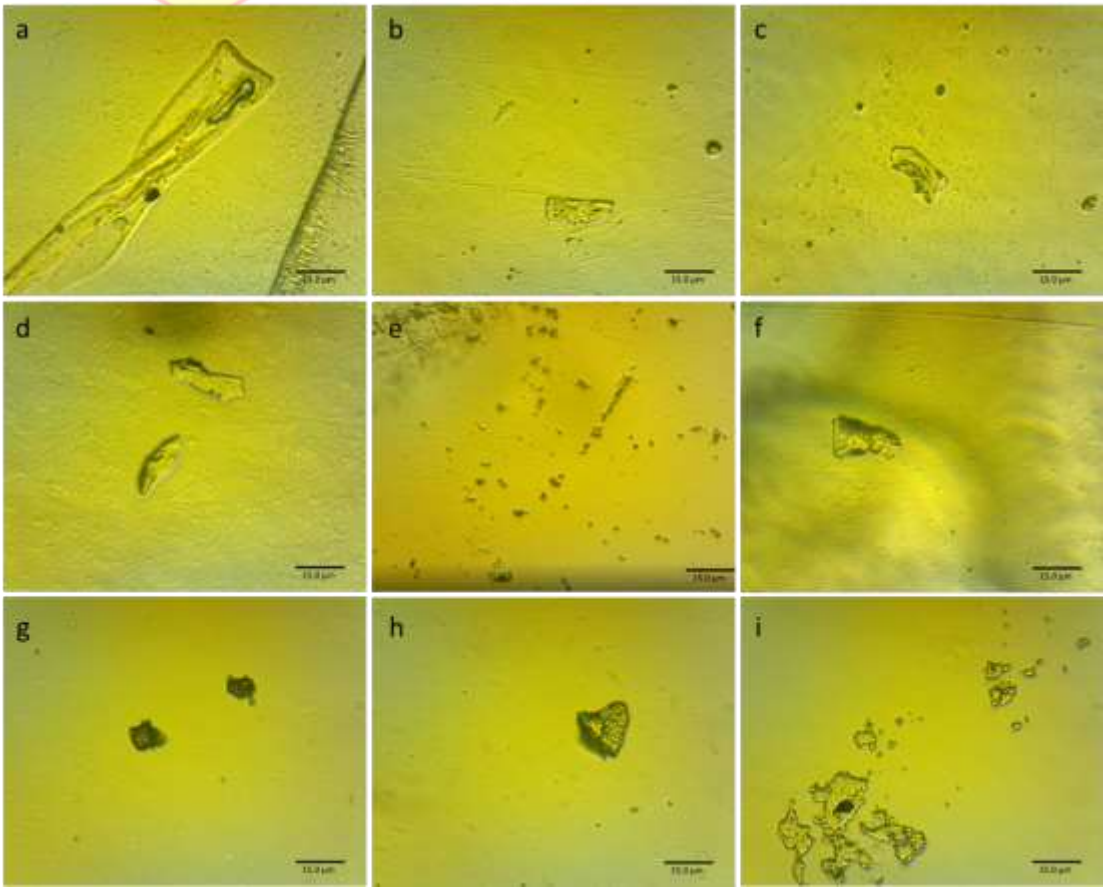

Figure 3.32. Representative inclusions found within Pfizer vaccine.

3.5.2. Raman Spectroscopic Investigation

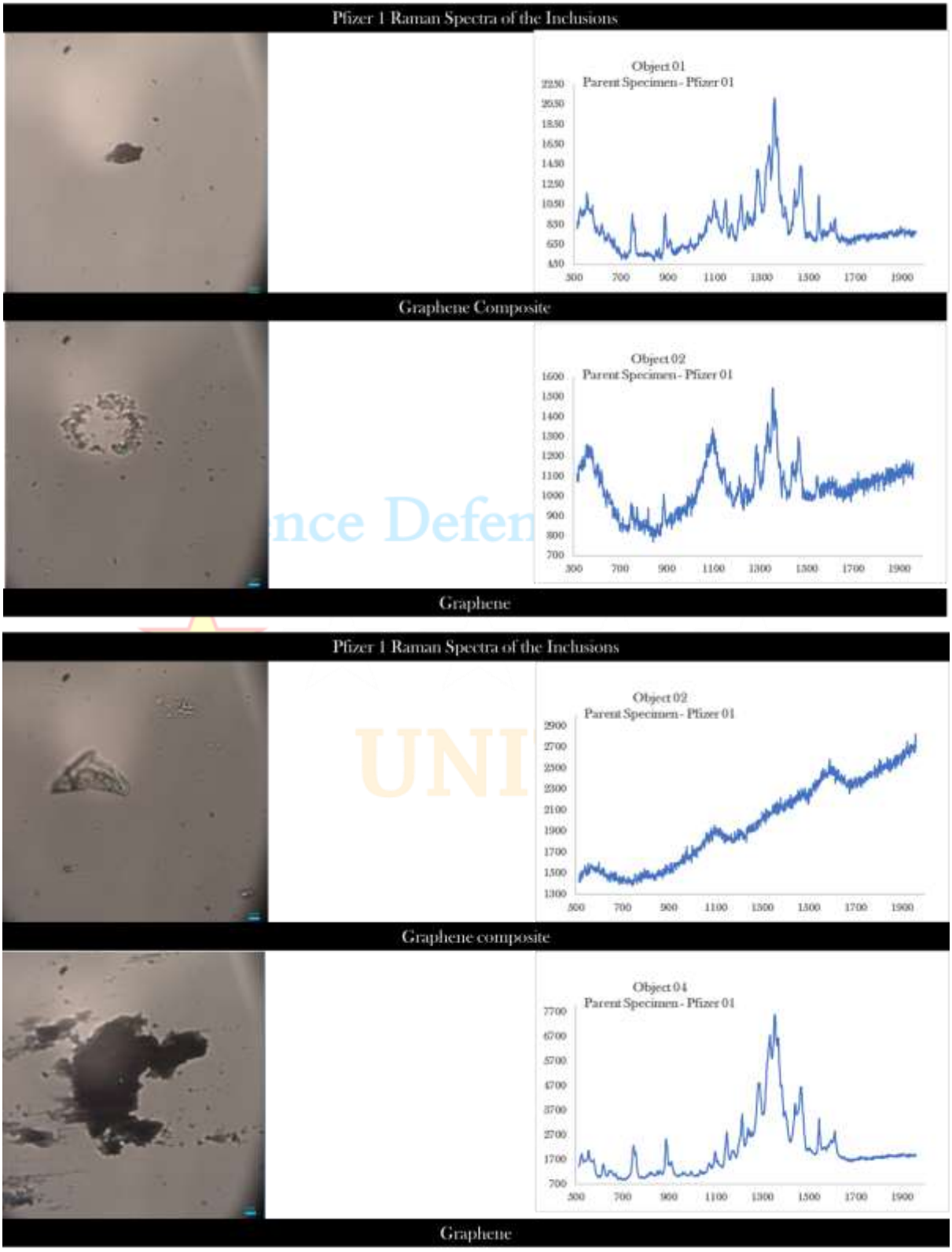

Figure 3.33. Raman spectra of various inclusions in AstraZeneca.

Raman spectroscopy was conducted on four selected representative samples for Pfizer (figure 3.32). Three of these samples showed carbon composite signatures with possible graphene in

them. The signals of amorphous carbon like materials were extremely complex with carbon along with iron oxide and several other compounds in them. The graphene complex 1 is graphene with polyethylene glycol signal forming the bulk of the spectrum. Though, for initial assessments, this study can confirm the presence of graphene in Pfizer, however, the complex with which it is associated still requires to be established through further work.

One of the sample that was shot, displayed a fair influence of fluorescence. Reshooting this sample at longer exposures is important to separate the signal from the article of interest with the signal of the background.

In summary, Raman helped identify the inclusions within Pfizer and these identifications were classed in the counts.

3.5.3. Counts

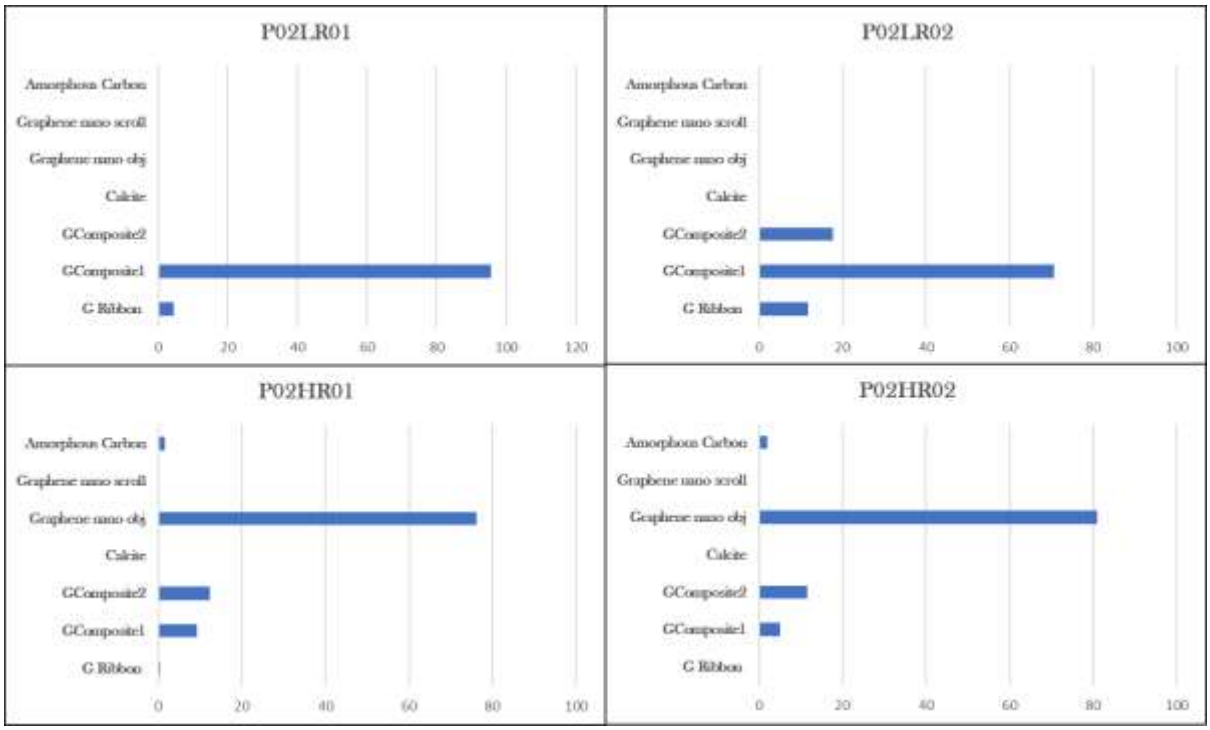

Figure 3.34. Count sheets at low and high resolutions along two tracks each for AstraZeneca.

The counts for Pfizer were conducted along four tracks of two each for Low and High magnifications (figure 3.34). The relative numbers of carbon composite 2 is quite high in one of the tracks whereas it is completely absent in the first track. At higher magnifications the counts are dominated by the sheer number of nano graphene objects.

It should be noted, that Graphene nano scrolls were omitted in the counts. This step was necessary because though, these nano scrolls form a significant percentage of the total counts, a confirmation of their composition could not be attained within the limitations of this project. As mentioned above in Section 3.1.5, thorough investigation of these forms now constitutes the subject of enhanced second investigation project following this report.

4. Interpretation, Discussions and Conclusion

Table 1
List of declared ingredients for the vaccines.

Moderna

Active Ingredients
- mRNA

Vehicles
- SM102
- Polyethylene Glycol
- 2000 dimyristoyl glycerol (DMG)
- Cholesterol
- 1,2-distearoyl-sn-glycero-3phosphocholine (DSPC)

Inactive Ingredients
- Tromethmine
- Tromethamine hydrochloride
- Acetic Acid
- Sodium Acetate
- Sucrose

AstraZeneca

Active Ingredients
- Adenovirus

Vehicles
- L-histidine
- L-histidine hydrochloride monohydrate

Inactive Ingredients
- Magnesium Chloride Hexahydrate
- Polysorbate 80
- Ethanol
- Sucrose
- Sodium Chloride
- Disodium edetate dihydrate (EDTA)
- Water

Pfizer

Active Ingredients
- mRNA

Vehicles
- 4-hydroxybutyl azanediyl bis hexane -6.1-diyl bis 2 hexyldecanoate
- Polyethylene Glycol
- N,N di tetra decylacetamide
- 1,2 di stearoyl sn glycerol 3phosphocholine
- Cholesterol

Inactive Ingredients
- Potassium Chloride
- Monobasic Potassium Phosphate
- Sodium Chloride
- Dibasic sodium, phosphate dehydrate
- Sucrose.

The study subjects were four vaccine samples (2 of Moderna, 1 of AstraZeneca and 1 of Pfizer). The objective of this study was to examine these four vaccine vials and document any undeclared ingredients in the composition of the vaccines, with special focus on graphene and related products as well as any biological forms.

It should be noted, that all three vaccines have very different chemical ingredients as declared by the manufacturers (Table 1). Despite, this genetic difference between them, upon examination, the results reveal common undeclared inclusions in the four vials.

These inclusions are primarily with a focus on graphene and carbon related nano structures in form of carbon or graphene composites, graphene in association with polyethylene glycol, graphene oxide, iron oxide compounds, and calcite. The variation in shapes of the logged inclusions, points to their varied purposes in the wider arena of drug delivery and biosensory fields.

The shapes identified during the course of this project can be classified into five different categories-

1. Ribbon Forms (G-PEG)
2. Sheet forms (GC-1)
3. Tubular forms (GC-2)
4. Nano Dots
5. Nano Scrolls

Where, the roles of the Ribbons and sheets remain unclear due to their microscopic sizes, the tubular forms along with nano dots and scrolls seem to be aimed at enhancing cell acceptance for the drug.

All three vaccines commonly employ the self-assembling lipid nano particles as drug delivery mechanisms. Where, the central find of this project has been the confirmation of the presence of graphene in all four samples, it is important to evaluate this find in the context of the subject itself.

As mentioned above, self-assembly processes are the core delivery mechanisms for the three types of vaccines. As has been reported under observations in the Chapter 3, the process in itself, is primarily dependent on weak intermolecular interactions (Mendes et al. 2013) which, in the case of lipid nanoparticles is driven and determined by the kinetics and the thermodynamic environment. However, based on the observations within this study, to kickstart the nucleation or seeding of these particles in the first state, Graphene nanoparticles

seem to play an important role. This interpretation is drawn from the observation that each of the nanoparticles seem to have a graphene core made of nano particles that float in the beginning and then saltate prior to settling down. This process creates a defect in the solution medium thereby, facilitating the formation of the nano particle seed. Given, the high concentration of graphene nano objects in all four vaccines, as the nanoparticles move through the medium, they must be incorporating not only graphene nanodots, but also nano scrolls, thereby increasing their binding efficiency and their ability to carry their pay load.

As is already well known, the structure of the lipid nano particle plays a crucial role in determining its efficiency to carry the nucleic acid payload. However, it is the payload's structure that defines the geometry of the lipid nanoparticles (Hajj et al. 2019, Kulkarni et al. 2018).

Though, these structures can be varied, depending upon the payload itself, the core responsibilities of the nano lipid particles are the same; viz (1) protection of nucleic acids from nucleases, (2) controlled release of nucleic acid, (3) cell and tissue selectivity, (4) high delivery yield, (5) minimal toxicity, and (6) stability especially in long-term storage. These required characteristics for a vector can been enhanced significantly by use of carbon nanotubes, graphene and graphene oxide. This process was observed in action, when the experiments were being conducted during the course of this study and as reported in detail within in Chapter 3.

Nano tubes, both single and multiwalled, along with graphene forms are increasingly, paving their way into targeted drug delivery (Sattari et al. 2021, Wu et al. 2018, Wierzbicki 2017, Eatemadi et al. 2014). The samples evaluated during the course of this project have identified graphene and other carbon composites as forming a striking percent portion of the ingredients of these vaccines. Given the context of the increasing use of graphene in drug delivery, the findings of this project seem to fit in the reference frame of attempts towards enhanced and tailored drug delivery.

The work carried out so far has been essentially a qualitative assessment of the contents. There are several forms within these vaccines that require quantitative assessment and determination. A major hurdle in achieving a good quantitative result was the failure to isolate the solid faction. The method used in this project was the traditional method of slide preparation. It is

hoped, that if similar work were to be performed on additional samples, vacuum filtering would be adopted as a mechanism of attaining cleaner samples for both Raman and SEM imaging.

Further, it is quite important to mention, that the source of fluorescence within the samples was unknown while Raman investigations were underway. Due to extremely tight timescales, it was not possible to complete the Raman re-runs where the effects of fluorescence would have been removed through targeted emittance and processing of the data. Despite this, the signals were interpreted using similar data from various catalogues. It is hoped that further work will continue on the Raman spectroscopic investigations to attain cleaner spectra and to isolate the individual spectrums of the current specimens.

In conclusion, it can be stated that the four samples of vaccines (Moderna 1, Modern 2, AstraZeneca, Pfizer) all contain significant amount of carbon composites, graphene compounds and iron oxide. These ingredients were undeclared by the manufacturers and are absent from the list of ingredients for the vaccines.

5. Bibliography

- Bonneville, S., Delpomdor, F., Preat, A., Chevaller,C., Arkaki, T., Kazemlan, M., Steele, A., Schrelber, A., Wirth, R., Benning, L.G. (2020). Molecular identification of fungi microfossils in a Neoproterozoic shale rock. Palentology, 6, 1-11.
- Buzgar, N. and Apopei, A. (2009). The Raman study of certain carbonates. Analele stiintifice ale univesrsitatii, al. i. cuza iasi. Geologie. Tomul LV, 2.
- Brennan, T.V., Lin, L., Huang, X. and Yang, Y. (2018). Generation of Luciferase-expressing Tumor Cell Lines. Bioprotocol, 8(8), 1-1
- Childres, I., Jauregui, L.A., Park, W., Cao, H. and Chen, Y.P. Raman spectroscopy of Graphene and related materials. Chapter 19.
- Crystal, R.G. (2014). Adenovirus: The First Effective In Vivo Gene Delivery Vector. Human Gene Therapy 25,3-11.
- Das, A., Chakraborty, B. and Sood, A.K. (2008). Raman Spectroscopy of graphene on different subsrates and influence of defects. Bulletin of Material Sciences, 31, 3, 579-584.
- Doerfler, W. (2021). Adenoviral Vector DNA- and SARS-CoV-2 mRNA-Based Covid-19 Vaccines: Possible Integration into the Human Genome – Are Adenoviral Genes Expressed in Vector -based Vaccines.
- Dychalska, A., Popielarski, P., Frankow, W., Fabisiak, K., Paprocki, K. and Szybowicz. (2015). Study of CVD diamond layers with amorphous carbon admixture by Raman scattering spectroscopy. Materials Science-Poland.
- Ghosh, S., Calizo, I., Teweldebrhan, D., Pokatilov, E.P., Nika, D.L., Balandin, A.A., Bao, W., Miao, F. and Lau, C.N. (2008). Extremely high thermal conductivity of graphene: Prospects for thermal management applications in nanoelectronic circuits. Applied Physics Letters, 92, 151911-1-3.
- Griffith, W.P. (1969). Raman spectroscopy of Minerals. Nature, 244, 264-266.
- Guo, W., Chen, Z., Feng, X., Shen, G., Huang, H., Liang, Y., Zhao, B., Lo, G. and Hu, Y. (2021). Graphene oxide (GO)- based nanosheets with combined chemo/photothermal/photodynamic therapy to overcome gastric cancer (GC) paclitaxel resistance by reducing mitochondria-derived adenonsine-triphosphate (ATP).
- Haskin, L.A., Wang, A., Rockow, K.M., Jolliff, B.L., Korotev, R.L. and Viskupic, K.M. (1997). Raman spectroscopy for mineral identification and quantification for insitu

planetary surface analysis: A point count method. Journal of Geophysical Research, 102, 8. 19293-19306.

- Hajj, A., Ball, R.L., Deluty, S.B., Singh, S.R., Strelkova, D., Knapp, C.M., Whitehead, K. (2019) Branched-tail lipid nanoparticles potently deliver mRNA in vivo due to enhanced ionization at endosomal pH. Small, 15,1–7.
- Jiao, L., Zhang, L., Wang, X., Diankov, G. and Dai, H. (2009). Narrow graphene nanoribbons from carbon nanotubes. Nature Letter, 458, 877-880.
- Jiang, W., Liang, F., Wang, J., Su, L., Wu, Y and Wang, L. (2014). Enhanced electrochemical performances of FeO – graphene nanocomposite as anode materials for alakaline nickel-iron batteries. **RSC Adv.**, 2014,**4**, 15394-15399.
- Kato, M., Guan, S. and Zhao, X. (2021). In-situ observation of graphene using an optical microscope. Applied Surface Science Advances, 6,
- Kim, J., Eygeris, Y., Gupta, M. and Sahay, G. (2021). Self-assembled mRNA vaccines. Advanced Drug Delviery Review, 170, 83-112.
- Kulkarni, A., Darjuan, M.M., Mercer, J.E., Chen, S., van der Meel, R., Thewalt, J.L., Tam, Y.Y.C., and Cullis, P.R. (2018). On the formation and morphology of lipid nanoparticles containing ionizable cationic lipids and siRNA. ACS Nano, 12, 4787–4795.
- Kuzmin, V.V., Novikov, V.S., Ustynyuk, L.Y., Prokhorov, K.A., Sagitova, E.A. and Nikolaeva, G.Y. (2020). Raman Spectra of polyethylene glycols: Comparative experimental and DFT study. Journal of Molecular Structure, 1217, 5,
- Liu, J., Cui, L. and Losic, D. (2013). Graphene and Graphene oxide as new nanocarriers for drug delivery applications. Acta Biomaterialia, 9(22).
- Malard, L.M., Pimenta, M.A., Desselhaus, G., Dresselhaus, M.S. (2009). Raman spectroscopy in graphene. Physics Reports, 473, 51-87.
- Mendes, A.C., Baran, E.T., Reis, R.L. and Azevedo, H.S. (2013). Self-assembly in nature: Using the principles of nature to create complex nanobiomaterials. Wiley Interdiscip Rev. Nanomed. Nanobiotechnol 5, 582-612.
- Osvath, Z., Zambo, D., Sulyok, A., Palinkas, A. and Deak, A. 2021. Tuning the nanoparticle rippling of graphene with PEGylated gold nanoparticles and ion radiation. Carbon Trends, 5, 1-5.
- Paillard, V. (2001). On the origin of the 1100cm^{-1} Raman band in amorphous and nanocrystalline sp^3 carbon. Europhysics Letters, 54(2), 194-198.

- Pierna, J.A.F., Abbas, O., Dardenne,P. and Baeten, V. (2011). Discrimination of Corsican honey by FT-Raman spectroscopy and chemometrics. Biotechnological Agron. Society Environment, 15,1, 75-84.
- Pop, E., Varshney, V., Roy, A. (2012). Thermal properties of graphene: Fundamentals and applications. MRS Bulletin 37, 1273-1281
- Prawer,S and Nemanich, R.J. (2004). Raman Spectroscopy of diamond and doped diamond. Philosophical Transactions of the Royal Society of London. Series A. Mathematical, Physical and Engineering Sciences. 362, 2537- 2565.
- Romann, J., Valmalette, J.C., Chevallier, V. and Merlen, A. (2010). Surface interactions between moleules and nanocrystals in copper oxalate nanostructures. Journal of Physical Chemistry, C. 114, 10677-19682.
- Roy, S. and Jaiswal, A. (2017). Graphene-based nanomaterials for theranostic applications. Reports in Advances of Physical Sciences, 1,4, 53pp.
- Sagitova, E.A., Prokhorov, K.A., Nikolaeva, G.Y., Baimova, A.V., Pashinin, P.P., Yarysheva, A.Y. and Mendeleev, D.I. (2018). Raman analysis of polyethylene glycols and polyethylene oxides. Journal of Physics Conference Series. 999 012002, 1-10.
- Sharma, S.K., Misra, A.K., Ismail, S. and Singh,U.N. (2006). Remote Raman Specroscopy of Various Mixed and Composite Mineral Phases at 7.2m Distance. https://www.researchgate.net/publication/252521525.
- Tallant, D.R., Friedmann, T.A., Missert, N.A., Siegal, M.P. and Sullivan, J.P. (1998). Raman spectroscopy of amorphous carbon. Material Research Society Symposium Proceedings, 498, 37-47.
- Zhao, X., Liu, L., Li, X., Zeng, J., Jia, X. and Liu P. (2014). Biocompatible graphene oxide nanoparticle-based drug delivery platform for tumor microenvironment-responsive triggered release of doxorubicin. Langmuir, 30(34),
- Wierzbicki, M., Jaworski, S., Kutwin, M., Grodzik, M., Strojny, B., Kurantowicz, N., Zdunek, K., Chodun, R., Chwalibog, A., Sawosz, E. (2017). Diamond, graphite and graphene oxide nanoparticles decrease migration and invasiveness in glioblastoma celllines by impairing extracellular adhesion. International Journal of Nanomedicine, 12, 7241-7254.
- Wu, J., Phillips, J.A., Liu, H. and Tan, Y.W.(2008). Carbon nanotubes protect DNA strnds during cellular delivery. ACS Nano.2 (2008) 2023-2028.

- Xie, W., Xu, G. and Feng, X. (2012). Self-assembly of lipid nano particles in aqueous solution; Self-consistent field simulations. Theoretical and Applied Mechanics Letters, 2, 014004, 1-5.
- Yong Tai, M.J., Perumal, V., Gopinath, S.C.B., Raja, P.B., Ibrahimm M.N.M., Jantan, I.N., Suhaimi, N.S.H. and Liu, W.W. (2021). Laser-scribed graphene nanofiber decorated with oil palm lignin capped silver nanoparticles: a green biosensor. Scientific Reports, 11,5475.